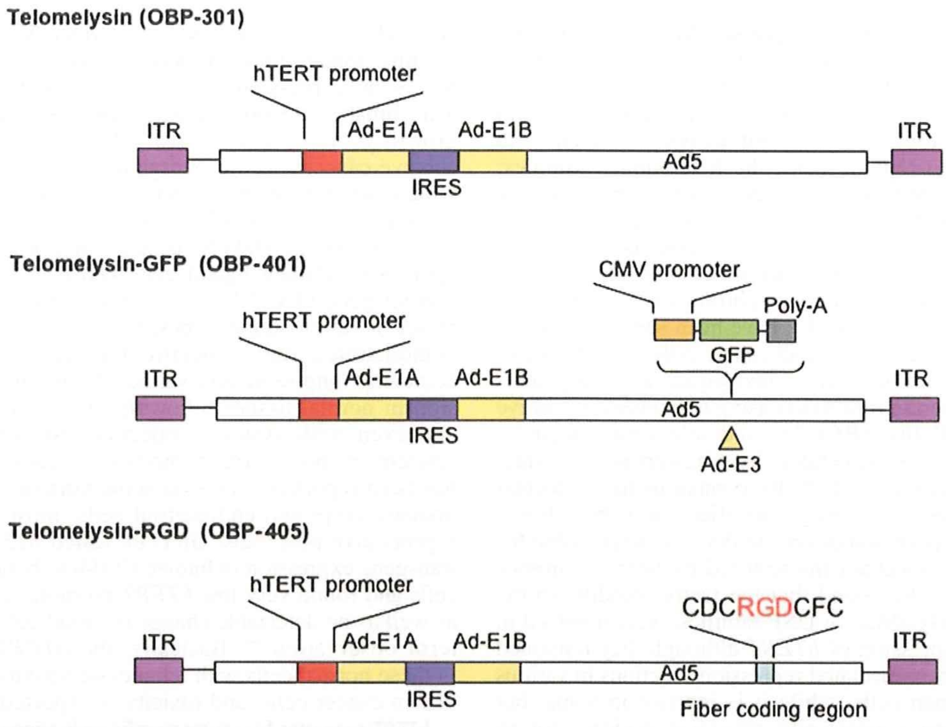

Fig. 2. Schematic DNA structures of telomerase-specific oncolytic viruses. Telomelysin (OBP-301) has *E1A* and *E1B* genes linked with an *IRES*, driven by the human telomerase reverse transcriptase (*hTERT*) promoter. A variant of OBP-301 was constructed that has the green fluorescent protein (*GFP*) gene at the *E3* region driven by *CMV* promoter (OBP-401). Another variant (OBP-405) has a mutant fiber containing the RGD peptide in the HI loop of the fiber knob.

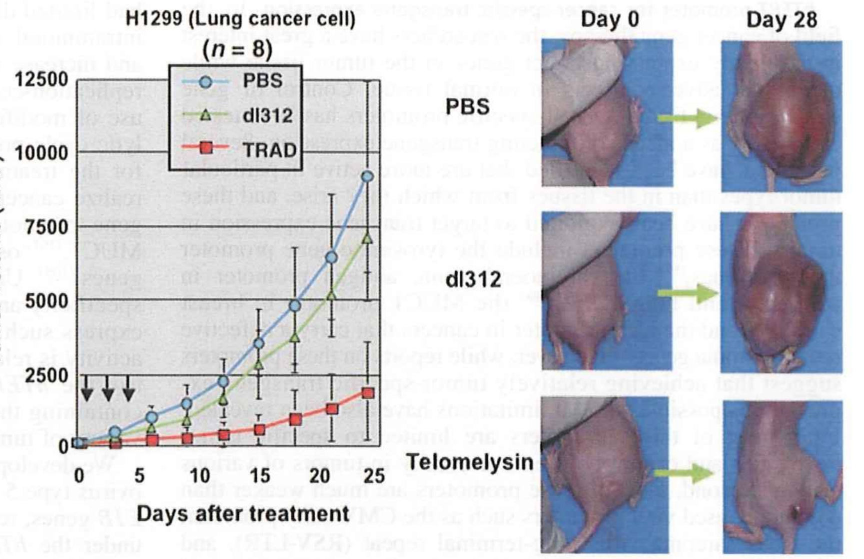

Fig. 3. *In vivo* effect of Telomelysin on tumorigenesis. Lung cancer H1299 cells were inoculated to the flank of nu/nμ mice. Mice bearing palpable tumors with a diameter of 5–6 mm received intratumoral injection of 10^7 PFU of Telomelysin or replication-deficient adenovirus (dL312) or phosphate-buffered saline (PBS) (mock treatment) on three consecutive days. The macroscopic appearances of H1299 tumors in nu/nμ mice at 0, 14, and 28 days after the treatment are shown. Note that the tumor growth was severely retarded by the treatment with Telomelysin. A modified version of this figure appeared in our original article.[106]

in cultured normal cells.[106,110] We confirmed that the transduction efficiency did not greatly differ in cancer and normal cells. Therefore, such difference in replication was considered to be due to the tumor specificity of Telomelysin. Since hTERT expression is observed broadly in a variety of tumor types, Telomelysin was expected to replicate in various cancer cells. Indeed, Telomelysin could efficiently kill head and neck, lung, esophageal, pancreatic, hepatic, prostate, and cervical cancers, as well as melanoma, sarcoma, and mesothelioma cells.[106,110]

The *in vivo* antitumor effect of Telomelysin was further investigated using mouse xenografts. Intratumoral injection of Telomelysin into inoculated tumors effectively retarded tumor growth and extended the survival of mice (Fig. 3). Telomelysin was also effective in progressive tumors with large tumor burden. When Telomelysin was directly injected to xenograft tumors after maximum growth, their size apparently decreased with the formation of massive ulceration at the site of injection.[106,110]

One technical merit for the use of replicative adenovirus is the unlimited replicative potential of virus over tumor mass. After tumor lysis due to viral toxicity, replicated viral particles can be released from tumors and spread to the whole body via blood or lymphatic flow[106] and finally replicate again at metastatic sites if they are telomerase-positive. Thus, in theory, Telomelysin might have efficacy against not only primary lesions but also metastatic sites.

Administration of Telomelysin in combination with chemotherapeutic agents. To enhance the therapeutic potential of Telomelysin, efforts have been made to combine it with several chemotherapeutic agents. Combination with docetaxel, vinorelbine (Nevelbine), or SN38 (active metabolite of irinotecan) has been confirmed *in vitro* to enhance Telomelysin cytotoxicity in different organs including the lung, colon, esophagus, stomach, liver, and prostate.[111] Of particular interest were the synergistic effects of Telomelysin when it was administrated intratumorally to xenografts in combination with intraperitoneal administration of docetaxel. The mechanism of this synergism remains unclear at present, but residual viable cells that survived after the treatment with docetaxel permit the replication of Telomelysin, leading to effective cell death. Telomerase-dependent virotherapy has also been shown to overcome tumor resistance against chemotherapy in hepatocellular carcinoma.[112]

HDAC inhibitors increase *Coxsackie's-adenovirus receptor* (*CAR*) gene expression in various cancer cell lines.[113] In addition, they are known to increase viral and transgene expression following adenovirus infection.[113] In fact, FR901228, a potent HDAC inhibitor, activated CAR levels on target tumor cells, increasing the amounts of Telomelysin replication, leading to synergistic antitumor effects.[114] Selection of the partner chemotherapeutic agents appears to be an important factor that affects and determines the efficacy of telomerase-dependent oncolytic virotherapy.

Clinical trial of Telomelysin. A phase I clinical trial of Telomelysin as monotherapy has been performed in the United States. The proposed protocol 'A phase I dose-escalation study of intratumoral injection with telomerase-specific replication-competent oncolytic adenovirus, Telomelysin (OBP-301) for various solid tumors', sponsored by Oncolys BioPharma, is an open-label, phase I, three-cohort dose-escalation study. The trial commenced following the approval of the US Food and Drug Administration (FDA) in October 2006. The study is still underway and we plan to assess the safety, tolerability, and feasibility of intratumoral injection of the agent in patients with advanced cancer. We will also analyze the humoral immune response to Telomelysin, and take tissue biopsies to evaluate the pharmacokinetics and pharmacodynamics of Telomelysin in the injected tumor. The therapeutic response will be assessed by measuring changes in tumor dimensions, comparative analysis of tumor biopsies, and cytokine and/or viral measurements. Patients selected for this trial have histologically or cytologically proven nonresectable solid tumors and have failed to respond to conventional therapies such as primary external beam radiation or systemic chemotherapy. All patients have a disease that is measurable and accessible to direct injection of Telomelysin. The doses of Telomelysin will be escalated from low to high virus particles in 1-log increments. Patients will be treated with a single intratumoral injection of Telomelysin and then monitored for 1 month.

hTERT promoter for cancer diagnostics

A novel approach has been developed to visualize cancer cells using cancer-specific replication-competent adenovirus expressing the green fluorescent protein (GFP). Telomelysin was modified to contain the *GFP* gene driven by the cytomegalovirus (*CMV*) promoter in the E3-deleted region[115] (Fig. 2). The resultant adenovirus was termed TelomeScan or OBP-401. TelomeScan replicated 5–6 orders of magnitude by 3 days after infection in human cancer cell lines and coordinately induced GFP expression. In contrast, it replicated only 2 orders of magnitude in normal human fibroblasts without significant GFP expression. When TelomeScan was directly injected to subcutaneous xenografts of human cancer cells, the xenografts exhibited GFP signals over their entire area and were easily visualized, indicating that TelomeScan had replicated and spread throughout the tumors (Fig. 4a).

Adenoviral spread and subsequent replication at distal sites may also be useful to visualize the metastatic foci of cancers. Theoretically, replicated TelomeScan can pass through the lymphatic pathway from the primary tumors to the regional or sentinel lymph nodes and can replicate in metastatic foci. To this end, *in vivo* experiments were performed using colorectal tumor models which were orthotopically implanted into the rectum in mice.[116] This mouse model shows para-arotic lymph node metastasis after implantation, which was histologically confirmed. Some para-arotic lymph nodes exhibited GFP signals 24 h after intratumoral injection of TelomeScan into the primary site. Lymph nodes with GFP signals were dissected, followed by histological examination, and were found to have metastatic foci of the tumor cells, while those without GFP signals had no metastatic foci (Fig. 4b). The sensitivity and specificity of this imaging technique to detect metastatic foci are 92.3% and 86.6%, respectively.

This *in vivo* imaging model may be useful during surgical lymphadenectomy. After injecting TelomeScan into the primary tumor, the surgeon can visualize metastatic lymph nodes with GFP fluorescence by illuminating the abdominal cavity with a Xenon lamp. Of course, this diagnostic modality may also be applied as therapeutic modality. We confirmed that TelomeScan has lesser but still sufficient cytotoxic effects compared with Telomelysin (data not shown). Therefore, injected TelomeScan that spreads to the regional lymph nodes or other metastatic foci may have the ability to eradicate any remaining tumor cells that the surgeon fails to completely remove.

Finally, we are currently using TelomeScan as a tool to visualize cancer cells in cytological samples. Once exfoliated cells obtained from certain tissues are infected, the TelomeScan can replicate preferentially in *hTERT*-promoter-positive cancer cells and exhibit GFP signals that can easily been detected by fluorescent microscopy (Fig. 4c) (Maida *et al.*, manuscript in preparation).

Conclusion and perspectives

In the past decade, a number of factors that regulate *hTERT* transcription have been identified. However, no single factor accounts for the cancer-specific expression of *hTERT*. It is obvious that multiple factors are involved in its regulation, probably in combination, and chromatin remodeling appears to play a critical role. It is of particular interest that active chromatin marks present around the transcription start site of the *hTERT* promoter are tightly associated with unmethlated DNA in hTERT-positive cells, suggesting a mechanism that is consistent with the usual dynamics of gene regulation via DNA methylation. DNA methylation and modification of nucleosome histones such as acethylation and methylation are functionally linked and cooperate to regulate chromatin structure and gene expression. Emerging evidence suggests that some of the histone methyltransferases directly target the *hTERT* promoter. Studies of *hTERT* promoter regulation will be developed in relation to chromatin remodeling factors.

Clinical application of *hTERT* promoter as a driving promoter in oncolytic adenovirus has been realized in the past 5 years. Although several oncolytic adenoviruses have been developed, Telomelysin is the first hTERT-dependent oncolytic adnovirus to be used in a clinical trial. Several barriers appear to limit the efficacy of Telomelysin, probably including some tumor types being refractory to infection with Telomelysin due to low CAR expression, as well as the adverse effects on normal hTERT-positive cells. Revised Telomelysin, termed Telomelysin-RGD or OBP-405, has been developed, in which the virus fiber was modified to contain RGD (Arg-Gly-Asp) peptide, which binds with high affinity to integrins on the cell surface, leading to increased infectivity. We should consider the fact that some

doi: 10.1111/j.1349-7006.2008.00878.x

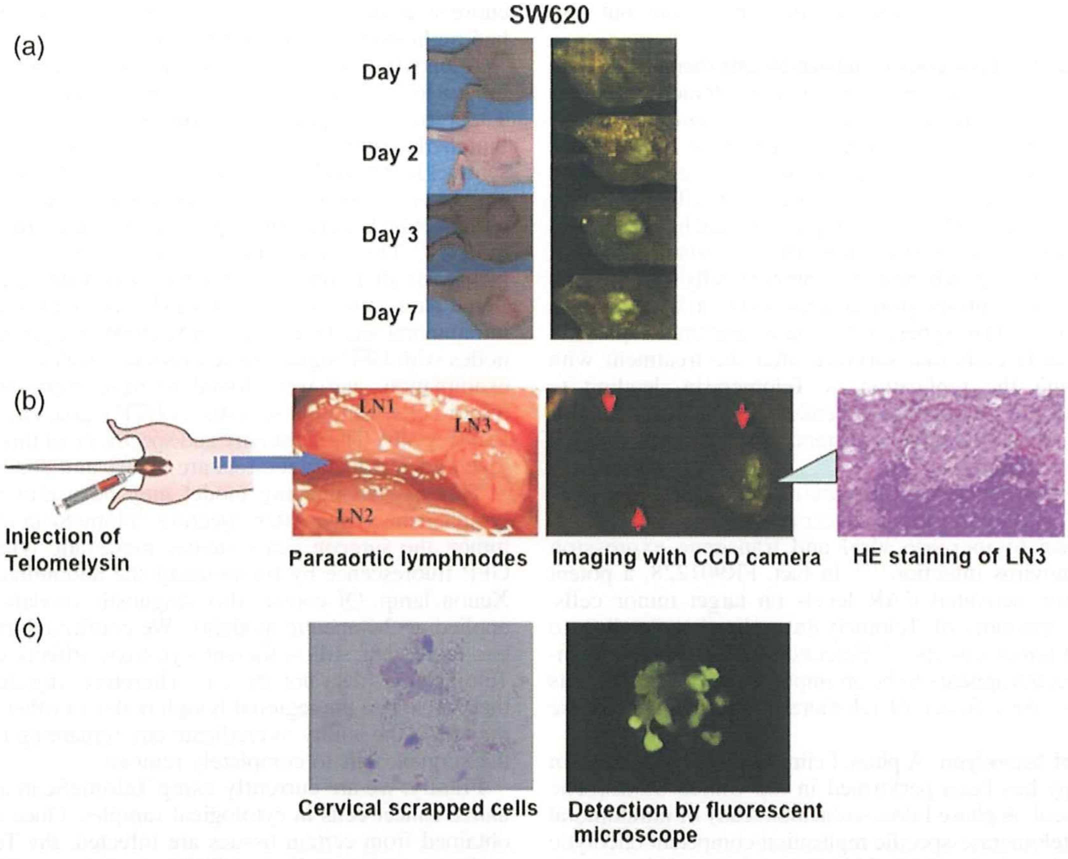

Fig. 4. Diagnostic utility of TelomeScan. (a) Visualization of tumor by the injection of TelomeScan. Subcutaneous tumor xenografts by colon cancer (SW620) were directly injected by TelomeScan at concentrations of 8×10^6 PFU. The green fluroescent protein (GFP) fluorescence intensity was monitored for seven consecutive days under the cooled charged-coupled device (CCD) imaging system. Left panels, macroscopic appearance of subcutaneous tumors; right panels, fluorescence detection. A modified version of this figure appeared in our original article.(114) (b) Selective visualization of lymph node metastasis by TelomeScan in orthotopic xenografts model. The rectums of mice were implanted with mouse rectal cancer HT29 cells. TelomeScan was directly injected into implanted tumor at a concentration of 1×10^8 PFU. At 5 days after the injection, mice were assessed for lymph node metastasis by laparotomy. Three swelled para-aortic lymph nodes were identified (LN1, LN2, and LN3). Internal imaging with the optical CCD camera showed one of the three nodes with GFP fluorescence (LN3), while the other lymph nodes (LN1, LN2) did not show (arrowheads indicate the position of swelled lymph nodes). Hematoxylin–eosin staining of lymph node sections revealed the apparent metastasis in LN3, while no metastatic sites were identified in LN1 or LN2 (data not shown), indicating that GFP fluorescence by the replication of TelomeScan is a potential biomaker of lymph node metastasis. A modified version of this figure appeared in our original article.(115) (c) Application of TelomeScan to visualization of cervical cancer cells in cytological samples. Uterine cervical scraping cells from patients with cervical cancer were incubated with TelomeScan at 10 MOI for 24 h, and then observed under light microscopy (left panel) or fluorescent microscopy (right panel). Clusters with cellular atypia exhibit GFP fluorescence.

normal cells, including some tissue stem cells, express relatively high levels of telomerase,(35,36,117) raising questions regarding the safety of Telomelysin. Although we have to wait for the final report of the clinical trial, no significant adverse effects on normal tissues have been reported so far, even in hematopoietic cells, which may be highly susceptible to Telomelysin due to the presence of telomerase-positive stem cells.(35) How can we explain such favorable phenomena? One possible explanation is that the hTERT promoter activity itself appears to be relatively lower in telomerase-positive normal cells than in hTERT-positive cancer cells, which limits its replication in normal cells and may largely contribute to the safety of this virus. Alternatively, Telomelysin may have lower capacity for infecting to hematopoietic stem cells possibly due to low CAR expression.(118)

Key to success of hTERT-dependent oncolytic virothrapy as a novel agent for cancer is a means of combining it with conventional therapies such as chemotherapy, radiotherapy, immunotherapy, surgery, or recently established molecular target therapies. The best combination and the timing of Telomelysin treatment (neoadjuvant, concurrent or adjuvant setting) should be investigated extensively in each tumor type.

Finally, diagnostic utility of hTERT-dependent oncolytic adenovirus for cancer may attract considerable attention in the near future. We began to apply this technology to cytological screening of cervical cancer and it should be extended to other tumor types for which cytological screening is important in early diagnosis. Intraoperative monitoring and detection of TelomeScan signals in the metastatic lymph nodes may provide revolutionary change in diagnostic modality during surgery. This novel technology will affect and contribute to the minimum operatin procedure for cancers.

Acknowledgments

This work was supported in part by Grants-in-Aid from the Ministry of Education, Science, and Culture of Japan; and grants from the Ministry of Health, and Welfare of Japan; and Megumi Medical Foundation at Kanazawa University, Japan. We greatly appreciate all members of the molecular pathology group in the Department of Obstetrics and Gynecology, Kanazawa University, for their devoted contribution to work on telomerase in human cancer. We also thank Mr Yasuo Urata, president of Oncolys BioPharma, Tokyo, Japan, for the collaborative setting of the clinical trial for Telomelysin.

References

1 Kim NW, Piatyszek MA, Prowse KR *et al.* Specific association of human telomerase activity with immortal cells and cancer. *Science* 1994; **266**: 2011–15.
2 Rudolph KL, Chang S, Lee HW *et al.* Longevity, stress response, and cancer in aging telomerase-deficient mice. *Cell* 1999; **96**: 701–12.
3 Chin L, Artandi SE, Shen Q *et al.* p53 deficiency rescues the adverse effects of telomere loss and cooperates with telomere dysfunction to accelerate carcinogenesis. *Cell* 1999; **97**: 527–38.
4 Artandi SE, DePinho RA. Mice without telomerase: what can they teach us about human cancer? *Nat Med* 2000; **6**: 852–5.
5 Meyerson M, Counter CM, Eaton EN *et al.* hEST2, the putative human telomerase catalytic subunit gene, is up-regulated in tumor cells and during immortalization. *Cell* 1997; **90**: 785–95.
6 Nakamura TM, Morin GB, Chapman KB *et al.* Telomerase catalytic subunit homologs from fission yeast and human. *Science* 1997; **277**: 955–9.
7 Bodnar AG, Ouellette M, Frolkis M *et al.* Extension of life-span by introduction of telomerase into normal human cells. *Science* 1998; **279**: 349–52.
8 Nakayama J, Tahara H, Tahara E *et al.* Telomerase activation by hTRT in human normal fibroblasts and hepatocellular carcinomas. *Nat Genet* 1998; **18**: 65–8.
9 Takakura M, Kyo S, Kanaya T, Tanaka M, Inoue M. Expression of human telomerase subunits and correlation with telomerase activity in cervical cancer. *Cancer Res* 1998; **58**: 1558–61.
10 Kyo S, Kanaya T, Takakura M, Tanaka M, Inoue M. Human telomerase reverse transcriptase as a critical determinant of telomerase activity in normal and malignant endometrial tissues. *Int J Cancer* 1999; **80**: 60–3.
11 Kanaya T, Kyo S, Takakura M, Ito H, Namiki M, Inoue M. *hTERT* is a critical determinant of telomerase activity in renal-cell carcinoma. *Int J Cancer* 1998; **78**: 539–43.
12 Kyo S, Kanaya T, Takakura M *et al.* Expression of human telomerase subunits in ovarian malignant, borderline and benign tumors. *Int J Cancer* 1999; **80**: 804–9.
13 Takakura M, Kyo S, Kanaya T *et al.* Cloning of human telomerase catalytic subunit (hTERT) gene promoter and identification of proximal core promoter sequences essential for transcriptional activation in immortalized and cancer cells. *Cancer Res* 1999; **59**: 551–7.
14 Horikawa I, Cable PL, Afshari C, Barrett JC. Cloning and characterization of the promoter region of human telomerase reverse transcriptase gene. *Cancer Res* 1999; **59**: 826–30.
15 Cong YS, Wen J, Bacchetti S. The human telomerase catalytic subunit hTERT. Organization of the gene and characterization of the promoter. *Hum Mol Genet* 1999; **8**: 137–42.
16 Wang J, Xie LY, Allan S, Beach D, Hannon GJ. Myc activates telomerase. *Genes Dev* 1998; **12**: 1769–174.
17 Wu KJ, Grandori C, Amacker M *et al.* Direct activation of TERT transcription by c-MYC. *Nature Genet* 1999; **21**: 220–4.
18 Greenberg RA, O'Hagan RC, Deng H *et al.* Telomerase reverse transcriptase gene is a direct target of c-Myc but is not functionally equivalent in cellular transformation. *Oncogene* 1999; **18**: 1219–26.
19 Kyo S, Takakura M, Taira T *et al.* Spl cooperates with c-Myc to activate transcription of the human telomerase reverse transcriptase gene (hTERT). *Nucleic Acids Res* 2000; **28**: 669–77.
20 Kirkpatrick KL, Ogunkolade W, Elkak AE *et al. hTERT* expression in human breast cancer and non-cancerous breast tissue: correlation with tumour stage and c-Myc expression. *Breast Cancer Res Treat* 2003; **77**: 277–84.
21 Günes C, Lichtsteiner S, Vasserot AP, Englert C. Expression of the hTERT gene is regulated at the level of transcriptional initiation and repressed by Mad1. *Cancer Res* 2000; **60**: 2116–21.
22 Xu D, Popov N, Hou M *et al.* Switch from Myc/Max to Mad1/Max binding and decrease in histone acetylation at the telomerase reverse transcriptase promoter during differentiation of HL60 cells. *Proc Acad Sci USA* 2001; **98**: 3826–31.
23 Deng WG, Jayachandran G, Wu G, Xu K, Roth JA, Ji L. Tumor-specific activation of human telomerase reverses transcriptase promoter activity by activating enhancer-binding protein-2beta in human lung cancer cells. *J Biol Chem* 2007; **282**: 26460–70.
24 Yatabe N, Kyo S, Maida Y *et al.* HIF-1-mediated activation of telomerase in cervical cancer cells. *Oncogene* 2004; **23**: 3708–15.
25 Nishi H, Nakada T, Kyo S, Inoue M, Shay JW, Isaka K. Hypoxia-inducible factor mediates upregulation of telomerase (hTERT). *Mol Cell Biol* 2004; **24**: 6076–83.
26 Koshiji M, Kageyama Y, Pete EA, Horikawa I, Barrett JC, Huang LE. HIF-1alpha induces cell cycle arrest by functionally counteracting Myc. *EMBO J* 2004; **23**: 1949–56.
27 Lou F, Chen X, Jalink M *et al.* The opposing effect of hypoxia-inducible factor-2alpha on expression of telomerase reverse transcriptase. *Mol Cancer Res* 2007; **5**: 793–800.
28 Takakura M, Kyo S, Inoue M, Wright WE, Shay JW. The function of AP1 on transcription of telomerase reverse transcriptase gene (TERT) in human and mouse cell. *Mol Cell Biol* 2005; **18**: 8037–43.
29 Kyo S, Takakura M, Kanaya T *et al.* Estrogen activates telomerase. *Cancer Res* 1999; **59**: 5917–21.
30 Misiti S, Nanni S, Fontemaggi G *et al.* Induction of hTERT expression and telomerase activity by estrogens in human ovary epithelium cells. *Mol Cell Biol* 2000; **20**: 3764–71.
31 Kimura A, Ohmichi M, Kawagoe J *et al.* Induction of hTERT expression and phosphorylation via Akt cascade by estrogen in human ovarian cancer cell lines. *Oncogene* 2004; **23**: 4505–15.
32 Wang Z, Kyo S, Maida Y *et al.* Tamoxifen regulates human telomerase reverse transcriptase (hTERT) gene expression differently in breast and endometrial cancer cells. *Oncogene* 2002; **21**: 3517–24.
33 Guo C, Armbruster BN, Price DT, Counter CM. *In vivo* regulation of hTERT expression and telomerase activity by androgen. *J Urol* 2003; **170**: 615–8.
34 Wang Z, Kyo S, Takakura M *et al.* Progesterone regulates human telomerase reverse transcriptase (hTERT) gene expression via activation of MAP kinase signaling pathway. *Cancer Res* 2000; **60**: 5376–81.
35 Hiyama K, Hirai Y, Kyoizumi S *et al.* Activation of telomerase in human lymphocytes and hematopoietic progenitor cells. *J Immunol* 1995; **155**: 3711–5.
36 Kyo S, Takakura M, Kohama T, Inoue M. Telomerase activity in human endometrium. *Cancer Res* 1997; **57**: 610–14.
37 Holt SE, Wright WE, Shay JW. Regulation of telomerase activity in immortal cell lines. *Mol Cell Biol* 1996; **16**: 2932–9.
38 Maida M, Kyo S, Kanaya T *et al.* Direct activation of telomerase by EGF through Ets-mediated transactivation of TERT via MAP kinase signaling pathway. *Oncogene* 2002; **21**: 4071–9.
39 Yang H, Kyo S, Takakura M, Sun L. Autocrine transforming growth factor b suppresses activity and hTERT transcription in human cancer cells. *Cell Growth Differ* 2001; **12**: 119–27.
40 Cerezo A, Kalthoff H, Schuermann M, Schäfer B, Boukamp P. Dual regulation of telomerase activity through c-Myc-dependent inhibition and alternative splicing of hTERT. *J Cell Sci* 2002; **115**: 1305–12.
41 Hu B, Tack DC, Liu T, Wu Z, Ullenbruch MR, Phan SH. Role of Smad3 in the regulation of rat telomerase reverse transcriptase by TGFbeta. *Oncogene* 2006; **25**: 1030–41.
42 Li H, Xu D, Li J, Berndt MC, Liu JP. Transforming growth factor beta suppresses human telomerase reverse transcriptase (hTERT) by Smad3 interactions with c-Myc and the hTERT gene. *J Biol Chem* 2006; **281**: 25588–600.
43 Lin SY, Elledge SJ. Multiple tumor suppressor pathways negatively regulate telomerase. *Cell* 2003; **113**: 881–9.
44 Lacerte A, Korah J, Roy M, Yang XJ, Lemay S, Lebrun JJ. Transforming growth factor-beta inhibits telomerase through SMAD3 and E2F transcription factors. *Cell Signal* 2008; **20**: 50–9.
45 Dyson N, Howley PM, Münger K, Harlow E. The human papilloma virus-16, E7 oncoprotein is able to bind to the retinoblastoma gene product. *Science* 1989, 243: 934–7.
46 Werness BA, Levine AJ, Howley PM. Association of human papillomavirus types 16 and 18E6 proteins with p53. *Science* 1990; **248**: 76–9.
47 Scheffner M, Huibregtse JM, Vierstra RD, Howley PM. The HPV-16 E6 and E6-AP complex functions as a ubiquitin-protein ligase in the ubiquitination of p53. *Cell* 1993; **75**: 495–505.
48 Scheffner M, Werness BA, Huibregtse JM, Levine AJ, Howley PM. The E6 oncoprotein encoded by human papillomavirus types 16 and 18 promotes the degradation of p53. *Cell* 1990; **63**: 1129–36.
49 Klingelhutz AJ, Foster SA, McDougall JK. Telomerase activation by the E6 gene product of human papillomavirus type 16. *Nature* 1996; **380**: 79–82.
50 Wang J, Xie LY, Allan S, Beach D, Hannon GJ. Myc activates telomerase. *Genes Dev* 1998; **12**: 1769–74.
51 Oh ST, Kyo S, Laimins LA. Telomerase activation by HPV-16 E6: induction of hTERT expression through Myc and GC-rich Spl binding sites. *J Virol* 2001; **75**: 5559–66.
52 Gewin L, Galloway DA. E box-dependent activation of telomerase by human papillomavirus type 16, E6 does not require induction of c-myc. *J Virol* 2001; **75**: 7198–201.
53 Veldman T, Horikawa I, Barrett JC, Schlegel R. Transcriptional activation of the telomerase hTERT gene by human papillomavirus type 16, E6 oncoprotein. *J Virol* 2001; **75**: 4467–72.
54 Gewin L, Myers H, Kiyono T, Galloway DA. Identification of a novel telomerase repressor that interacts with the human papillomavirus type-16, E6/E6-AP complex. *Genes Dev* 2004; **18**: 2269–82.
55 Goueli BS, Janknecht R. Upregulation of the catalytic telomerase subunit by the transcription factor ER81 and oncogenic HER2/Neu, ras, or raf. *Mol Cell Biol* 2004; **24**: 25–35.
56 Shin KH, Kang MK, Dicterow E *et al.* Hypermethylation of the hTERT promoter inhibits the expression of telomerase activity in normal oral fibroblasts and senescent normal oral keratinocytes. *Br J Cancer* 2003; **89**: 1473–8.

doi: 10.1111/j.1349-7006.2008.00878.x

57 Lopatina NG, Poole JC, Saldanha SN *et al.* Control mechanisms in the regulation of telomerase reverse transcriptase expression in differentiating human teratocarcinoma cells. *Biochem Biophys Res Commun* 2003; **306**: 650–9.
58 Liu L, Saldanha SN, Pate MS *et al.* Epigenetic regulation of human telomerase reverse transcriptase promoter activity during cellular differentiation. *Genes Chromosomes Cancer* 2004; **41**: 26–37.
59 Devereux TR, Horikawa I, Anna CH, Annab LA, Afshari CA, Barrett JC. DNA methylation analysis of the promoter region of the human telomerase reverse transcriptase (hTERT) gene. *Cancer Res* 1999; **59**: 6087–90.
60 Dessain SK, Yu H, Reddel RR, Beijersbergen RL, Weinberg RA. Methylation of the human telomerase gene CpG island. *Cancer Res* 2000; **60**: 537–41.
61 Guilleret I, Yan P, Grange F, Braunschweig R, Bosman FT, Benhattar J. Hypermethylation of the human telomerase catalytic subunit (hTERT) gene correlates with telomerase activity. *Int J Cancer* 2002; **101**: 335–41.
62 Zinn RL, Pruitt K, Eguchi S, Baylin SB, Herman JG. hTERT is expressed in cancer cell lines despite promoter DNA methylation by preservation of unmethylated DNA and active chromatin around the transcription start site. *Cancer Res* 2007; **67**: 194–201.
63 Stein GS, Montecino M, van Wijnen AJ, Stein JL, Lian JB. Nuclear structure-gene expression interrelationships: implications for aberrant gene expression in cancer. *Cancer Res* 2000; **60**: 2067–76.
64 Cong YS, Bacchetti S. Histone deacetylation is involved in the transcriptional repression of hTERT in normal human cells. *J Biol Chem* 2000; **275**: 35665–8.
65 Takakura M, Kyo S, Sowa Y *et al.* Telomerase activation by histone deacetylase inhibitor in normal cells. *Nucleic Acids Res* 2001; **29**: 3006–11.
66 Doetzlhofer A, Rotheneder H *et al.* Histone deacetylase 1 can repress transcription by binding to Sp1. *Mol Cell Biol* 1999; **19**: 5504–11.
67 Suzuki T, Kimura A, Nagai R, Horikoshi M. Regulation of interaction of the acetyltransferase region of p300 and the DNA-binding domain of Sp1 on and through DNA binding. *Genes Cells* 2000; **5**: 29–41.
68 Oh S, Song YH, Yim J, Kim TK. Identification of Mad as a repressor of the human telomerase (hTERT) gene. *Oncogene* 2000; **19**: 1485–90.
69 Atkinson SP, Hoare SF, Glasspool RM, Keith WN. Lack of telomerase gene expression in alternative lengthening of telomere cells is associated with chromatin remodeling of the hTR and hTERT gene promoters. *Cancer Res* 2005; **65**: 7585–90.
70 Liu C, Fang X, Ge Z *et al.* The telomerase reverse transcriptase (hTERT) gene is a direct target of the histone methyltransferase SMYD3. *Cancer Res* 2007; **67**: 2626–31.
71 Kanaya T, Kyo S, Hamada K *et al.* Adenoviral expression of p53 represses telomerase activity through down-regulation of human telomerase reverse transcriptase transcription. *Clin Cancer Res* 2000; **6**: 1239–47.
72 Xu D, Wang Q, Gruber A *et al.* Downregulation of telomerase reverse transcriptase mRNA expression by wild type p53 in human tumor cells. *Oncogene* 2000; **19**: 5123–33.
73 Oh S, Song Y, Yim J, Kim TK. The Wilms' tumor 1 tumor suppressor gene represses transcription of the human telomerase reverse transcriptase gene. *J Biol Chem* 1999; **274**: 37473–8.
74 Fujimoto K, Kyo S, Takakura M *et al.* Identification and characterization of negative regulatory elements of the human telomerase catalytic subunit (hTERT) gene promoter: possible role of MZF-2 in transcriptional repression of hTERT. *Nucleic Acids Res* 2000; **28**: 2557–62.
75 Ikeda N, Uemura H, Ishiguro H *et al.* Combination treatment with 1alpha, 25-dihydroxyvitamin D3 and 9-cis-retinoic acid directly inhibits human telomerase reverse transcriptase transcription in prostate cancer cells. *Mol Cancer Ther* 2003; **2**: 739–46.
76 Oshimura M, Barrett JC. Multiple pathways to cellular senescence: role of telomerase repressors. *Eur J Cancer* 1997; **33**: 710–5.
77 Horikawa I, Oshimura M, Barrett JC. Repression of the telomerase catalytic subunit by a gene on human chromosome 3 that induces cellular senescence. *Mol Carcinogen* 1998; **22**: 65–72.
78 Tanaka H, Shimizu M, Horikawa I, Kugoh H, Yokota J, Barrett JC, Oshimura M. Evidence for a putative telomerase repressor gene in the 3p14.2-p21.1 region. *Genes Chromosomes Cancer* 1998; **23**: 123–33.
79 Cuthbert AP, Bond J, Trott DA *et al.* Telomerase repressor sequences on chromosome 3 and induction of permanent growth arrest in human breast cancer cells. *J Natl Cancer Inst* 1999; **91**: 37–45.
80 Ducrest AL, Amacker M, Mathieu YD *et al.* Regulation of human telomerase activity: repression by normal chromosome 3 abolishes nuclear telomerase reverse transcriptase transcripts but does not affect c-Myc activity. *Cancer Res* 2001; **61**: 7594–602.
81 Backsch. C, Wagenbach N, Nonn M *et al.* Microcell-mediated transfer of chromosome 4 into HeLa cells suppresses telomerase activity. *Genes Chromosomes Cancer* 2001; **31**: 196–8.
82 Steenbergen RDM, Kramer D, Meijer CJ *et al.* Telomerase suppression by chromosome 6 in a human papillomavirus type 16-immortalized keratinocyte cell line and in a cervical cancer cell line. *J Natl Cancer Inst* 2001; **93**: 865–72.
83 Nakabayashi K, Ogino H, Michishita E, Satoh N, Ayusawa D. Introduction of chromosome 7 suppresses telomerase with shortening of telomeres in a human mesothelial cell line. *Exp Cell Res* 1999; **252**: 376–82.
84 Nishimoto A, Miura N, Horikawa I *et al.* Functional evidence for a telomerase repressor gene on human chromosome 10p15.1. *Oncogene* 2001; **20**: 828–35.
85 Yang X, Tahin Q, Hu YF *et al.* Functional roles of chromosomes 11 and 17 in the transformation of human breast epithelial cells *in vitro*. *Int J Oncol* 1999; **15**: 629–38.
86 Horikawa I, Cable PL, Mazur SJ, Appella E, Afshari CA, Barrett JC. Downstream E-box-mediated regulation of the human telomerase reverse transcriptase (hTERT) gene transcription: evidence for an endogenous mechanism of transcriptional repression. *Mol Biol Cell* 2002; **13**: 2585–97.
87 Vile RG, Hart IR. In vitro and in vivo targeting of gene expression to melanoma cells. *Cancer Res* 1993; **53**: 962–7.
88 Osaki T, Tanio Y, Tachibana I *et al.* Gene therapy for carcinoembryonic antigen-producing human lung cancer cells by cell type-specific expression of herpes simplex virus thymidine kinase gene. *Cancer Res* 1994; **54**: 5258–61.
89 Chen L, Chen D, Manome Y, Dong Y, Fine HA, Kufe DW. Breast cancer selective gene expression and therapy mediated by recombinant adenoviruses containing the DF3/MUC1 promoter. *J Clin Invest* 1995; **96**: 2775–82.
90 Parr MJ, Manome Y, Tanaka T *et al.* A. Tumor-selective transgene expression in vivo mediated by an E2F-responsive adenoviral vector. *Nat Med* 1997; **3**: 1145–9.
91 Gu J, Kagawa S, Takakura M *et al.* Tumor-specific transgene expression from hTERT promoter: targeting pharmaceutical effects of the Bax gene to cancer. *Cancer Res* 2000; **60**: 5359–64.
92 Komata T, Koga S, Hirohata S *et al.* A novel treatment of human malignant gliomas in vitro and in vivo: FADD gene transfer under the control of the human telomerase reverse transcriptase gene promoter. *Int J Oncol* 2001; **19**: 1015–20.
93 Koga S, Hirohata S, Kondo Y *et al.* FADD gene therapy using the human telomerase catalytic subunit (hTERT) gene promoter to restrict induction of apoptosis to tumors in vitro and in vivo. *Anti Cancer Res* 2001; **21**: 1937–43.
94 Komata T, Kondo Y, Kanzawa T *et al.* Treatment of malignant glioma cells with the transfer of constitutively active caspase-6 using the human telomerase catalytic subunit (hTERT) gene. *Cancer Res* 2001; **61**: 5796–802.
95 Takeuchi H, Kanzawa T, Kondo Y *et al.* Combination of caspase transfer using the human telomerase reverse transcriptase promoter and conventional therapies for malignant glioma cells. *Int J Oncol* 2004; **25**: 57–63.
96 Takeda T, Inaba H, Yamazaki M *et al.* Tumor-specific gene therapy for undifferentiated thyroid carcinoma utilizing the telomerase reverse transcriptase promoter. *J Clin Endcrinol Metab* 2003; **88**: 3531–8.
97 Lin T, Huang X, Gu J *et al.* Long-term tumor-free survival from treatment with the GFP-TRAIL fusion gene expressed from the hTERT promoter in breast cancer cells. *Oncogene* 2002; **21**: 8020–8.
98 Nakamura M, Kyo S, Kanaya T *et al.* hTERT-promoter-based tumor specific expression of MCP-1 effectively sensitize cervical cancer cells to a low dose of cisplatin. *Cancer Gene Ther* 2004; **11**: 1–7.
99 Gu J, Andreeff M, Roth JA, Fang B. hTERT promoter induces tumor-specific Bax gene expression and cell killing in syngenic mouse tumor model and prevents systemic toxicity. *Gene Ther* 2002; **9**: 30–7.
100 Rodriguez R, Schuur ER, Lim HY, Henderson GA, Simons JW, Henderson DR. Prostate attenuated replication competent adenovirus (ARCA) CN706: a selective cytotoxic for prostate-specific antigen-positive prostate cancer cells. *Cancer Res* 1997; **57**: 2559–63.
101 Kurihara T, Brough DE, Kovesdi I, Kufe DW. Selectivity of a replication-competent adenovirus for human breast carcinoma cells expressing the MUC1 antigen. *J Clin Invest* 2000; **106**: 763–71.
102 Matsubara S, Wada Y, Gardner TA *et al.* A conditional replication-competent adenoviral vector, Ad-OC-E1a, to cotarget prostate cancer and bone stroma in an experimental model of androgen-independent prostate cancer bone metastasis. *Cancer Res* 2001; **61**: 6012–9.
103 Peng XY, Won JH, Rutherford T *et al.* The use of the 1-plastin promoter for adenoviral-mediated, tumor-specific gene expression in ovarian and bladder cancer cell lines. *Cancer Res* 2001; **61**: 4405–13.
104 Adachi Y, Reynolds PN, Yamamoto M *et al.* A midkine promoter-based conditionally replicative adenovirus for treatment of pediatric solid tumors and bone marrow tumor purging. *Cancer Res* 2001; **61**: 7882–8.
105 Tsukuda K, Wiewrodt R, Molnar-Kimber K, Jovanovic VP, Amin KM. An E2F-responsive replication-selective adenovirus targeted to the defective cell cycle in cancer cells: potent antitumoral efficacy but no toxicity to normal cell. *Cancer Res* 2002; **62**: 3438–47.
106 Kawashima T, Kagawa S, Kobayashi N *et al.* Telomerase-specific replication selective virotherapy for human cancer. *Clin Cancer Res* 2004; **10**: 285–92.
107 Wirth T, Zender L, Schulte B *et al.* A telomerase-dependent conditionally replicating adenovirus for selective treatment of cancer. *Cancer Res* 2003; **63**: 3181–8.

108 Lanson NA Jr, Friedlander PL, Schwarzenberger P, Kolls JK, Wang G. Replication of an adenoviral vector controlled by the human telomerase reverse transcriptase promoter causes tumor-selective tumor lysis. *Cancer Res* 2003; **63**: 7936–41.
109 Irving J, Wang Z, Powell S *et al.* Conditionally replicative adenovirus driven by the human telomerase promoter provides broad-spectrum antitumor activity without liver toxicity. *Cancer Gene Ther* 2004; **11**: 174–85.
110 Taki M, Kagawa S, Nishizaki M *et al.* Enhanced oncolysis by OBP-405, a tropism-modified telomerase-specific replication-selective adenoviral agent. *Oncogene* 2005; **24**: 3130–40.
111 Fujiwara T, Kagawa S, Kishimoto H *et al.* Enhanced antitumor efficacy of telomerase-selective oncolytic adenoviral agent OBP-401 with docetaxel: preclinical evaluation of chemovirotherapy. *Int J Cancer* 2006; **119**: 432–40.
112 Wirth T, Kühnel F, Fleischmann-Mundt B *et al.* Telomerase-dependent virotherapy overcomes resistance of hepatocellular carcinomas against chemotherapy and tumor necrosis factor-related apoptosis-inducing ligand by elimination of Mcl-1. *Cancer Res* 2005; **65**: 7393–402.
113 Kitazono M, Goldsmith ME, Aikou T, Bates S, Fojo T. Enhanced adenovirus transgene expression in malignant cells treated with the histone deacetylase inhibitor FR901228. *Cancer Res* 2001; **61**: 6328–30.
114 Watanabe T, Hioki M, Fujiwara T *et al.* Histone deacetylase inhibitor FR901228 enhances the antitumor effect of telomerase-specific replication-selective adenoviral agent OBP-301 in human lung cancer cells. *Exp Cell Res* 2006; **312**: 256–65.
115 Umeoka T, Kawashima T, Kagawa S *et al.* Visualization of intrathoracically disseminated solid tumors in mice with optical imaging by telomerase-specific amplification of a transferred green fluorescent protein gene. *Cancer Res* 2004; **64**: 6259–65.
116 Kishimoto H, Kojima T, Watanabe Y *et al.* A novel in vivo imaging of lymph node metastasis with telomerase-specific replication-competent adenovirus containing green fluorescent protein gene. *Nat Med* 2006; **12**: 1213–9.
117 Masutomi K, Yu EY, Khurts S *et al.* Telomerase maintains telomere structure in normal human cells. *Cell* 2003; **114**: 241–53.
118 Sakurai F, Mizuguchi H, Hayakawa T. Efficient gene transfer into human CD34[+] cells by an adenovirus type 35 vector. *Gene Ther* 2003; **10**: 1041–8.

doi: 10.1111/j.1349-7006.2008.00878.x

Oncogene (2008) 27, 2375–2381

www.nature.com/onc

ORIGINAL ARTICLE

Virus-mediated oncolysis induces danger signal and stimulates cytotoxic T-lymphocyte activity via proteasome activator upregulation

Y Endo[1,2], R Sakai[1,2], M Ouchi[3], H Onimatsu[3], M Hioki[1,2], S Kagawa[1,2], F Uno[1,2], Y Watanabe[3], Y Urata[3], N Tanaka[1] and T Fujiwara[1,2]

[1]Division of Surgical Oncology, Department of Surgery, Okayama University Graduate School of Medicine, Dentistry and Pharmaceutical Sciences, Okayama, Japan; [2]Center for Gene and Cell Therapy, Okayama University Hospital, Okayama, Japan and [3]Oncolys BioPharma Inc., Tokyo, Japan

Dendritic cells (DCs) are the most potent antigen-presenting cells and acquire cellular antigens and danger signals from dying cells to initiate antitumor immune responses via direct cell-to-cell interaction and cytokine production. The optimal forms of tumor cell death for priming DCs for the release of danger signals are not fully understood. OBP-301 (Telomelysin) is a telomerase-specific replication-competent adenovirus that induces selective E1 expression and exclusively kills human cancer cells. Here, we show that OBP-301 replication produced the endogenous danger signaling molecule, uric acid, in infected human tumor cells, which in turn stimulated DCs to produce interferon-γ (IFN-γ) and interleukin 12 (IL-12). Subsequently, IFN-γ release upregulated the endogenous expression of the proteasome activator PA28 in tumor cells and resulted in the induction of cytotoxic T-lymphocytes. Our data suggest that virus-mediated oncolysis might be the effective stimulus for immature DCs to induce specific activity against human cancer cells.
Oncogene (2008) **27,** 2375–2381; doi:10.1038/sj.onc.1210884; published online 5 November 2007

Keywords: adenovirus; telomerase; dendritic cell; uric acid; danger signal

Introduction

Dendritic cells (DCs) are the most important professional antigen-presenting cells and play a critical role in the induction of primary immune responses against tumor-associated antigens. Mature DCs express high levels of major histocompatibility complex (MHC) class I, II and co-stimulatory molecules such as CD80 and CD86, and secrete T-helper type-1 (Th1) cytokines such as interleukin (IL)-12 and interferon (IFN)-γ. DCs acquire endogenous maturation stimuli from dying cells as a danger signal when they capture cellular antigens. Lack of danger signals delays maturation of DCs and causes active suppression of DCs stimulatory capacity, leading to the induction of T-cell tolerance (Steinman *et al.*, 2000). Shi *et al.* (2003) have previously identified uric acid as a novel endogenous warning molecule capable of alerting the immune system within cell lysates. The uric acid activates DCs following relocation from the inside to the outside of injured cells and converts immunity from non-protective to protective. In fact, it has been reported that uric acid levels are elevated in tumors undergoing immune rejection and that the inhibition of uric acid production delays tumor regression (Hu *et al.*, 2004).

Viruses have evolved to infect, replicate in and kill human cells through diverse mechanisms such as direct cell death machinery and fairly brisk immune responses. We reported previously that telomerase-specific replication-competent adenovirus (Telomelysin, OBP-301), in which the human telomerase reverse transcriptase (hTERT) promoter element drives the expression of *E1A* and *E1B* genes linked with an internal ribosome entry site (IRES), induced selective E1 expression and efficiently killed human cancer cells, but not normal human fibroblasts (Kawashima *et al.*, 2004; Umeoka *et al.*, 2004; Taki *et al.*, 2005; Watanabe *et al.*, 2006). Although the precise molecular mechanism of OBP-301-induced cell death is still unclear, the process of oncolysis is morphologically distinct from apoptosis and necrosis. These findings led us to examine whether tumor cells killed by OBP-301 infection could stimulate DCs, thus enhancing the immune response.

In the present study, we compared three types of tumor preparations as a source of cell-derived antigen for the priming of DCs: virus-induced oncolysis, chemotherapeutic drug-induced apoptosis and necrosis by freeze/thaw. We also explored the cytokine signature and activating property of these cells for antitumor immune response against human cancer cells.

Results

We first examined whether OBP-301 infection affects the viability of human cancer cells using the XTT assay.

Correspondence: Dr T Fujiwara, Center for Gene and Cell Therapy, Okayama University Hospital, 2-5-1 Shikata-cho, Okayama 700-8558, Japan.
E-mail: toshi_f@md.okayama-u.ac.jp
Received 30 July 2007; revised 14 September 2007; accepted 17 September 2007; published online 5 November 2007

OBP-301 infection induced death of human cancer cell lines (H1299 human lung cancer and SW620 human colorectal cancer cells) in a dose-dependent manner (Figure 1). Although autophagy, or type II programmed cell death, partially involved in the cell death machinery triggered by OBP-301 infection, oncolytic cells are distinct from apoptotic cells (Supplementary Figure 1).

We next examined whether OBP-301 infection modulated intracellular concentrations of uric acid that might act as a danger signal in tumor cells. Uric acid levels increased in H1299 cells following OBP-301 infection in a time-dependent fashion, although docetaxel slightly upregulated the uric acid concentration 72 h after treatment (Figure 2a). Thus, tumor cells undergoing oncolysis can produce significantly greater amounts of uric acid when compared with apoptotic tumor cells. The uric acid elevation pattern of OBP-301-infected cells almost paralleled that of cells infected with Onyx-015, an E1B 55 kDa-deleted adenovirus engineered to selectively replicate in and lyse p53-deficient cancer cells, and wild-type adenovirus type 5 (Figure 2b), indicating a general effect of adenovirus infection in the regulation of intracellular uric acid levels.

Uric acid is produced during the catabolism of purines and is the end product of this process. Adenoviral replication facilitates the purine catabolism to stimulate the synthesis of progeny DNA, which in turn may increase intracellular uric acid levels by the purine degradation process. In fact, OBP-301 infection significantly increased the amount of uric acid in the cells, whereas replication-deficient dl312 infection had no apparent effect on the levels of uric acid. OBP-301-induced elevation of uric acid levels could be inhibited in the presence of cidofovir (CDV), an acyclic nucleoside phosphonate having potent broad-spectrum anti-DNA virus activity (Figure 2c). CDV has been approved for the treatment of many types of viruses including cytomegalovirus and adenovirus (Lenaerts and Naesens, 2006). We confirmed that CDV at 100 μM could significantly inhibited replication of OBP-301 in H1299 cells by the real-time quantitative PCR analysis (Supplementary Figure 2). Moreover, as OBP-301 replication was attenuated in telomerase-negative cells, the levels of uric acid could not be altered in normal human lung fibroblasts (NHLF) after OBP-301 infection (Figure 2d). These results suggest that viral replication is required to produce uric acid in infected cells.

Xanthine oxidoreductase (XOR) is a member of the molybdoflavoenzyme family that catalyses the formation of uric acid from xanthine and hypoxanthine (Glantzounis *et al.*, 2005). A strand-specific reverse transcriptase PCR assay demonstrated that XOR mRNA expression gradually decreased in OBP-301-infected cells presumably due to the negative feedback of increased uric acid levels, whereas docetaxel-treated cells yielded consistent bands of the XOR transcripts (Figure 2e). Thus, adenoviral replication could directly stimulate the catalytic DNA turnover, which enables cells to produce more uric acid.

We then examined the ability of OBP-301-infected cells to stimulate immature DCs *in vitro*. DCs generated from HLA-A24$^+$ healthy volunteers were co-cultured with HLA-matched H1299 cells (HLA-A32/A24) treated with OBP-301 or docetaxel for 72 h, or freeze thawed. The production of Th1 cytokines such as IFN-γ and IL-12 in the supernatants was then explored by enzyme-linked immunosorbent assay (ELISA) analysis 48 h after the coculture. DCs incubated with OBP-301-infected cells secreted large amounts of IFN-γ and IL-12, whereas stimulation with docetaxel-treated apoptotic cells induced their secretion at low levels (Figure 3a). The level of cytokine production from DCs incubated with freeze-thawed necrotic cells was similar to that of untreated immature DCs. Moreover, we confirmed that addition of OBP-301 alone without target tumor cells did not affect the cytokine secretion of DCs into the supernatant, indicating that infection of OBP-301 itself had no apparent effect on DCs. Thus, DCs stimulated with oncolytic tumor cells preferentially secrete high-level Th1 cytokines. Flow cytometry demonstrated that the increase in the expression of CD83, which is expressed on mature DCs, was slightly higher on DCs incubated with oncolytic cells than those with apoptotic or necrotic cells, indicating that oncolytic tumor cells seems to have a positive influence on DC maturation (Supplementary Figure 3).

In the next step, we investigated the effects of oncolytic tumor cells on T-cell activation in the presence of DCs. H1299 cells were infected with OBP-301 over 72 h, and then co-incubated with HLA-matched HLA-A24$^+$ peripheral blood mononuclear cells (PBMCs) for another 48 h in mixed lymphocyte tumor culture (MLTC). In other tests, H1299 cells were exposed to docetaxel for 72 h or freeze thawed, and then co-cultured with PBMCs. We examined the secretion of IFN-γ and IL-12 into the supernatants after MLTC for 7 days. Stimulation with OBP-301-infected cells induced the secretion of high levels of IFN-γ and IL-12 into MLTC supernatants, which was significantly higher

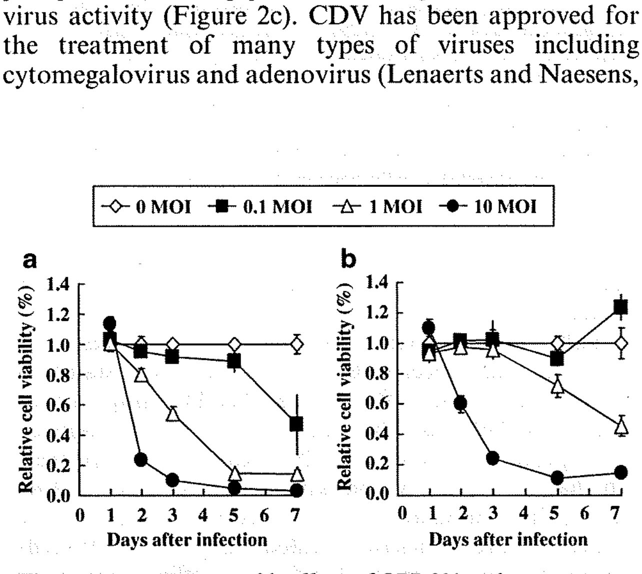

Figure 1 *In vitro* cytopathic effects of OBP-301 on human cancer cells. H1299 human non-small cell lung cancer (**a**) and SW620 human colorectal cancer cells (**b**) were infected with OBP-301 at indicated multiplicity of infection (MOI) values, and surviving cells were quantitated over 7 days by XTT assay. The cell viability of mock-treated cells on day 1 was considered 1.0, and the relative cell viability was calculated. Each data represent the mean ± standard deviation (s.d.) of triplicate experiments.

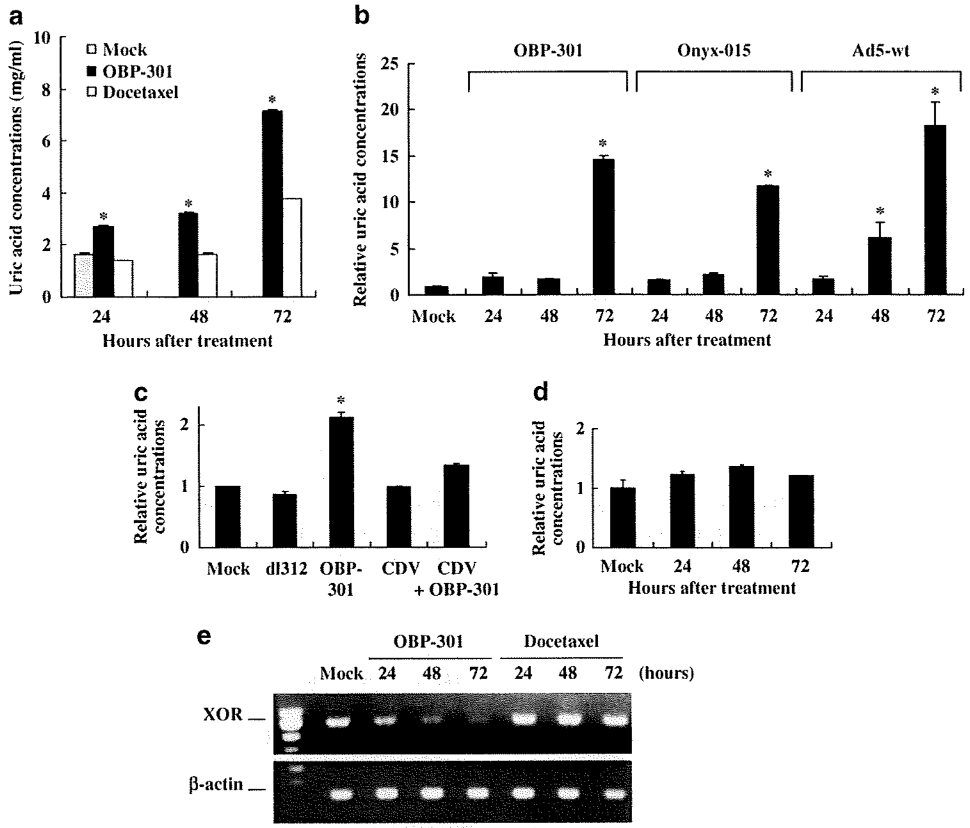

Figure 2 (**a**) Uric acid concentrations in H1299 cells treated with OBP-301 or docetaxel. H1299 cells were infected with 1.0 MOI of OBP-301 or treated with 10 nM of docetaxel for indicated time periods, and uric acid concentrations were determined enzymatically in the cell homogenates. Single asterisk indicates $P < 0.01$, significantly different from docetaxel-treated cells. (**b**) Uric acid levels in H1299 cells treated with OBP-301, Onyx-015 or wild-type adenovirus. H1299 cells were harvested at indicated time points over 72 h after infection with 10 MOI of viruses, and subjected to the measurement of uric acid concentrations. The levels of uric acid concentration are defined as the fold-increase for each sample relative to that of mock-treated cells (mock equals 1). Single asterisk indicates $P < 0.01$, significantly different from mock-treated cells. (**c**) Uric acid concentrations in H1299 cells infected with 1.0 MOI of OBP-301 or replication-deficient dl312 adenovirus were measured 24 h after infection. Uric acid production was also assessed in H1299 cells infected with 1.0 MOI of OBP-301 in the presence of 100 μM of anti-virus agent cidofovir (CDV). H1299 cells treated with 100 μM of CDV were subjected to the assay as a control. All uric acid levels are normalized to that of mock-treated cells (mock equals 1). (**d**) Uric acid levels in NHLF infected with OBP-301. NHLF cells were infected with 1.0 MOI of OBP-301 for indicated time periods, and uric acid concentrations were measured. The uric acid levels are normalized to that of mock-treated cells. (**e**) Detection of xanthine oxidoreductase (XOR) mRNA expression in OBP-301-infected H1299 cells by RT–PCR analysis. Cells were infected with 1.0 MOI of OBP-301 or treated with 10 nM of docetaxel, and then collected at the indicated time points. First-strand DNA generated from RNA was amplified using either the primers specific for XOR sequence or the primers that recognize β-actin sequences as an internal control.

than that with docetaxel-treated or freeze-thawed H1299 cells (Figure 3b). Thus, oncolytic tumor cells can accelerate the cleavage of tumor antigen peptides that can be associated with MHC class I molecules via IFN-γ secretion by immune cells.

Stimulation of cells with IFN-γ is known to induce the expression of PA28, a proteasome activator that accelerates the *in vitro* processing of MHC class I ligands from their polypeptide precursors (Sun *et al.*, 2002). We investigated whether PA28 expression was upregulated in H1299 cells by adding the supernatants of co-cultures of PBMCs and OBP-301-infected H1299 cells. Western blot analysis for PA28 demonstrated that, following heat inactivation of residual OBP-301, MLTC supernatants with oncolytic tumor cells induced a strong endogenous PA28 expression in H1299 cells. In contrast, exposure to the supernatants of PBMCs alone, PBMCs with untreated H1299 cells, and PBMCs with oncolytic tumor cells without heat inactivation resulted in no apparent changes in the expression levels of PA28 (Figure 4).

Finally, the cytotoxic T-lymphocyte (CTL) response against human cancer cells was assessed by a standard 6-h ^{51}Cr release assay after a 7-day MLTC using various forms of H1299 cells. The lytic activity of CTLs induced by apoptotic or necrotic H1299 cells was comparable with that of human lymphokine-activated killer (LAK) cells; CTLs stimulated with oncolytic H1299 cells, however, more efficiently killed target H1299 cells (Figure 5). In contrast, LAK cells effectively lysed SW620 cells, whereas these cells were minimally killed by CTLs stimulated with apoptotic, necrotic or oncolytic H1299 cells. Furthermore, HLA-unmatched, HLA-A26/A30$^+$ A549 human lung cancer cells were not sensitive to oncolytic tumor cell-induced cytotoxicity (data not shown), suggesting that effector cells stimulated with

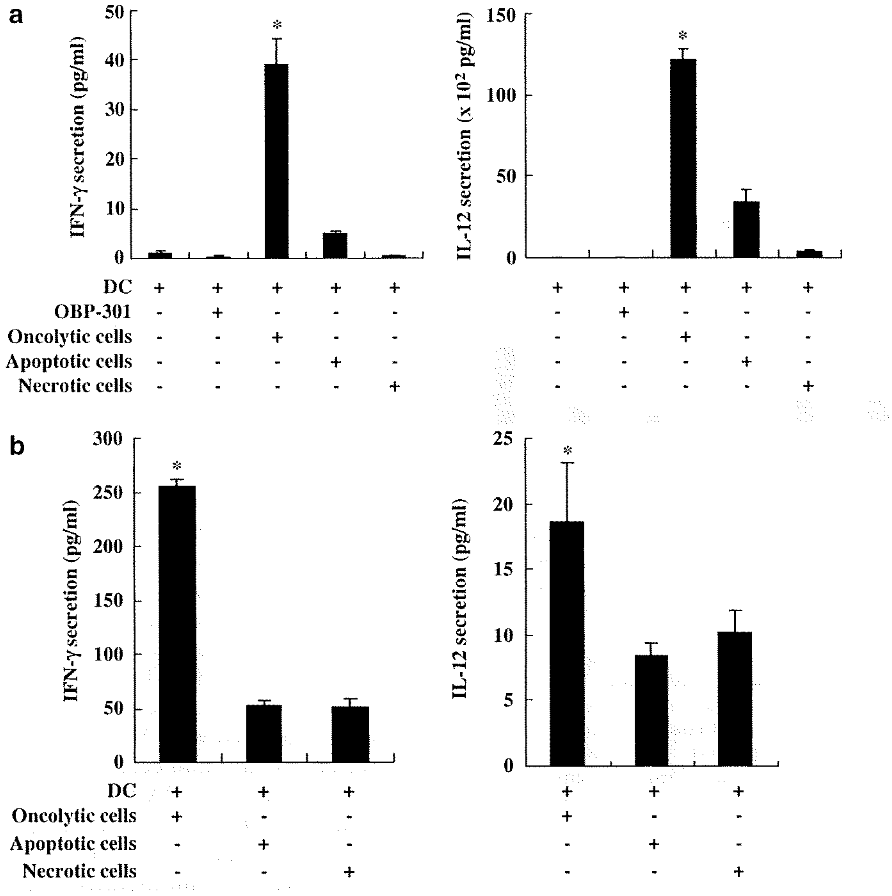

Figure 3 (**a**) Secretion of Th1-type cytokines by oncolytic, apoptotic or necrotic tumor cells. H1299 cells were treated with 1.0 MOI of OBP-301 or 50 nM of docetaxel for 72 h, or freeze thawed, and then co-cultured with immature dendritic cells (DCs) obtained from monocytes for additional 48 h. The culture supernatants were harvested and tested by ELISA for interferon (IFN)-γ (left) and interleukin (IL)-12 (right) concentrations. As a control, the supernatants of immature DCs alone or with OBP-301 at an MOI of 1.0 were also examined. Data are mean ± s.d. of triplicate experiments. Single asterisk indicates $P < 0.01$, significantly different from other groups. (**b**) Tumor-specific CTL induction in MTLC with oncolytic, apoptotic or necrotic tumor cells. IFN-γ (left) and IL-12 (right) concentrations in the supernatants of MLTC analysed by ELISA. H1299 cells were treated with 1.0 MOI of OBP-301 or 50 nM of docetaxel for 72 h, or freeze thawed, and then co-cultured with PBMCs obtained from HLA-A24^{-} healthy volunteers for 48 h in MLTC. Data are mean ± s.d. of triplicate experiments. Single asterisk indicates $P < 0.01$, significantly different from other groups.

OBP-301-infected tumor cells exhibit MHC class I-restricted reactivity.

Discussion

In the present study, our goal was to determine whether oncolytic virus is effective not only as a direct cytotoxic drug but also as an immunostimulatory agent that could induce specific CTL for the remaining antigen-bearing tumor cells. Several groups have debated whether necrotic or apoptotic cells can stimulate DCs to cross-present cell-derived peptides, with subsequent enhancement of tumor immunogenicity. Furthermore, it has been reported recently that the immunogenicity of tumors is not regulated by signals associated with apoptotic or necrotic cell death, but is an intrinsic feature of the tumor itself (Bartholomae *et al.*, 2004). Our data indicate that viral oncolysis could efficiently load tumor antigen on DCs, and then generate CTL response as judged from the production of cytokines. Moreover, the CTL activity against untreated tumor cells suggests that CTLs are specific to tumor antigens, but not to adenovirus proteins.

DCs are known to ingest dying tumor cells and initiate tumor-specific responses when associated with appropriate danger signals, which are endogenous activation signals liberated by dying cells. Recent studies have shown that some intrinsic biochemical factors, such as uric acid, bradykinin and heat shock protein (HSP110) act as danger signals through their interaction with DCs, and influence the subsequent immune response (Aliberti *et al.*, 2003; Shi *et al.*, 2003; Manjili *et al.*, 2005). Large amounts of uric acid can be produced following tissue injury *in vivo*, and activate the immune response against injured cells and dying tissues. We found that OBP-301 infection increased intracellular uric acid levels in human tumor cells compared with apoptosis- or necrosis-inducing stimuli, suggesting that viral replication itself can enhance tumorigenicity.

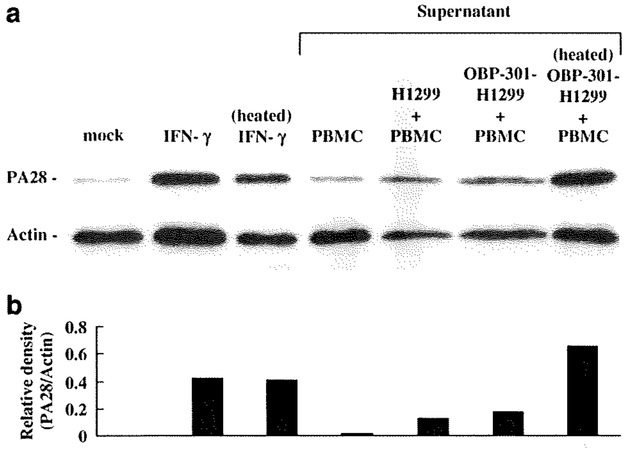

Figure 4 (**a**) Western blot analysis of PA28 in H1299 cells exposed to the supernatants of MLTC. peripheral blood mononuclear cells (PBMCs) were incubated with mock, untreated H1299 cells or H1299 cells treated with 10 MOI of OBP-301 for 72 h in MLTC, and the supernatants were harvested 48 h after the co-culture. H1299 cells were further incubated with the supernatants for 72 h with or without heat inactivation of residual virus (56 °C, 10 min). H1299 cells were also incubated with 5 ng ml^{-1} of interferon (IFN)-γ with or without heating for 72 h. Equivalent amounts of protein obtained from whole cell lysates were loaded in each lane, probed with anti-PA28 antibody and then visualized by using an ECL detection system. Equal loading of samples was confirmed by stripping each blot and reprobing with anti-actin antiserum. (**b**) PA28 protein expression was quantified by densitometric scanning using NIH Image software and normalization by dividing the actin signal.

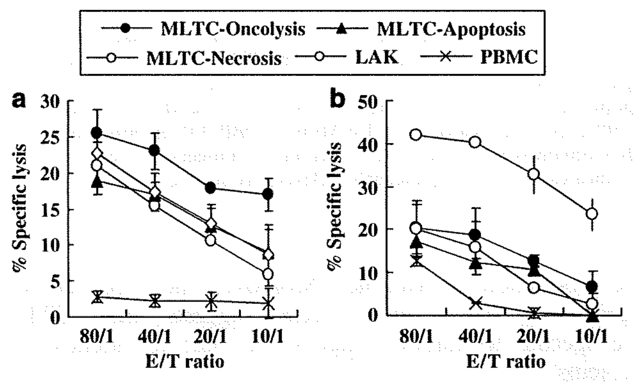

Figure 5 Cytolytic reactivity against H1299 (**a**) and SW620 (**b**) human cancer cells was assessed after 7-day mixed lymphocyte tumor culture (MLTC) with oncolytic, apoptotic or necrotic H1299 cells treated the same as above by 6-h standard ^{51}Cr-release assay. Lymphokine-activated killer (LAK) cells were generated from peripheral blood mononuclear cells (PBMCs) in the presence of interleukin (IL)-2 (100 U ml^{-1}) for 3 days. The CTLs were compared with LAK cells and untreated PBMCs, which served as positive and negative controls, respectively. Data represent the mean ± s.d. of three wells at four different effector-to-target (E/T) ratios.

Viral oncolysis increases the immunogenicity of tumor cells presumably by the release of proinflammatory cytokines (Lindenmann and Klein, 1967). We showed that OBP-301-infected oncolytic tumor cells efficiently stimulated immature DCs to produce greater amounts of IFN-γ and IL-12 than apoptotic and necrotic cells, and that such stimulation led to DC maturation. Viral infection itself has been reported to activate DCs to secrete pro- or anti-inflammatory cytokines, which can drive DCs to undergo the maturation process (Ho *et al*., 2001); the observation that OBP-301 alone had no effect on cytokine production by DCs, however, indicates that OBP-301 itself may be less infective or stimulatory to DCs. The result is consistent with our finding that OBP-301 attenuated replication as well as cytotoxicity in human normal cells.

It will be of interest to more mechanistically define why viral oncolysis efficiently induces CTL activity against tumor cells. We hypothesized that viral replication itself or the released cytokines by immune cells positively influences tumor cell immunogenicity. The IFN-γ-inducible proteasome modulator complex PA28 participates in the generation of antigenic peptides required for MHC class I antigen presentation (Sijts *et al*., 2002). As expected, the supernatants of MLTC with OBP-301-infected tumor cells, in which IFN-γ secretion was detected, induced a strong expression of endogenous PA28. Thus, oncolytic tumor cells can accelerate the cleavage of tumor antigen peptides that can be associated with MHC class I molecules via IFN-γ secretion by immune cells. In fact, it has been reported that restoration of PA28 expression in PA28-deficient melanoma cells rescues the melanoma antigen epitope presentation (Sun *et al*., 2002); our preliminary experiments however demonstrated that human tumor cells transfected with PA28α expression vector were less sensitive to tumor-specific CTLs (data not shown). These observations suggest that antigen peptide production alone does not seem sufficient to enhance tumor immunogenicity.

In conclusion, we provide for the first time evidence that oncolytic virus replication induces tumor-specific immune responses by stimulating uric acid production as a danger signal as well as accelerating tumor antigen cleavage by IFN-γ-inducible PA28 expression. Since the induction of systemic immunity has rarely been observed in clinical trials with other conditionally replication-competent viruses, more *in vivo* experiments are clearly required to support the induction of antitumor immunity by OBP-301 treatment. Our data, however, suggest that the antitumor effect of OBP-301 might be potentially both direct and indirect as well as systemic rather than local.

Materials and methods

Cell lines and reagents

The human non-small lung cancer cell lines H1299 (HLA-A32/A24) and the human colorectal carcinoma cell lines SW620 (HLA-A02/A24) were maintained *in vitro* in RPMI 1640 supplemented with 10% fetal calf serum, 100 U ml^{-1} penicillin and 100 mg ml^{-1} streptomycin. Recombinant human cytokines granulocyte/macrophage colony-stimulating factor (GM-CSF), IL-4, TNF-α and IL-7 were purchased from Genzyme

Techne (Minneapolis, MN, USA), IFN-γ from Peprotech (Rocky Hill, NJ, USA) and IL-2 from Roche (Mannheim, Germany). [^{51}Cr] sodium chromate was obtained from NEN Life Science Products (Boston, MA, USA). Docetaxel (taxotere) was kindly provided by Aventis Pharma (Tokyo, Japan).

Adenovirus

The recombinant replication-selective, tumor-specific adenovirus vector OBP-301 (Telomelysin), in which the hTERT promoter element drives the expression of *E1A* and *E1B* genes linked with an IRES, was constructed and characterized previously (Kawashima *et al.*, 2004; Umeoka *et al.*, 2004; Taki *et al.*, 2005; Watanabe *et al.*, 2006). Onyx-015 (dl1520) is an E1B 55 kDa-deleted adenovirus engineered to selectively replicate in and lyse p53-deficient cancer cells, and kindly provided by Dr Frank McCormick (UCSF Comprehensive Cancer Center and Cancer Research Institute). The E1A-deleted adenovirus vector lacking a cDNA insert (dl312) was also used as a control vector. The viruses were purified by $CsCl_2$ step gradient ultracentrifugation followed by $CsCl_2$ linear gradient ultracentrifugation.

Cell viability assay

XTT assay was performed to measure cell viability. Briefly, cells were plated on 96-well plates at 5×10^3 per well 24 h before treatment and then infected with OBP-301 or exposed to docetaxel. Cell viability was determined at the times indicated by using a Cell Proliferation Kit II (Roche Molecular Biochemicals) according to the protocol provided by the manufacturer.

Reverse transcription (RT)–PCR

Total RNA was isolated from mock-, OBP-301- and docetaxel-treated cells using RNAzol (Cinna/BioTecx, Friendswood, TX, USA) in a single-step phenol-extraction method and used as templates. Reverse transcription was performed at 22 °C for 10 min and then 42 °C for 20 min using 1.0 μg of RNA per reaction to ensure that the amount of amplified DNA was proportional to that of specific mRNA in the original sample. PCR was performed with specific primers in volumes of 50-μl according to the s protocol provided by the manufacturer (PCR kit; Perkin-Elmer/Cetus, Norwalk, CT, USA). The specific primers used for XOR were 5′-GCG AAG GAT AAG GTT ACT TGT-3′ (forward) and 5′-CTC CAG GTA GAA GTG CTC TTG-3′ (reverse); and for β-actin were 5′-ATG GTG GGA ATG GGT CAG AAG-3′ (forward) and 5′-GCA GCT CAT TGT AGA AGG-3′ (reverse). The reaction conditions were denaturing at 94 °C for 2 min followed by 30 cycles consisting of denaturing at 94 °C (30 s), annealing at 65 °C (15 s) and extension at 72 °C (10 s) using a thermal cycler (Perkin-Elmer, Foster City, CA, USA). The reactions were completed by a final 2-min extension at 72 °C. The PCR products were resolved on 1% agarose gels and visualized by SYBR Gold Nucleic Acid Gel Stain (Molecular Probes Inc., Eugene, OR, USA).

Preparation of tumor cells

For induction of oncolysis, tumor cells were infected with OBP-301 at a multiplicity of infection (MOI) of 1–10, and then collected 24–72 h after infection. Apoptotic tumor cells were obtained after 24–72-h exposure to 50–100 nM of docetaxel. For induction of necrosis, tumor cells suspended in phosphate-buffered saline (PBS) were subjected to rapid four freeze/thaw cycles using a 60 °C water bath and liquid nitrogen.

Measurement of uric acid concentration

Cultured cells were harvested after treatment and rinsed three times with PBS. These cells were resuspended in lysis buffer at a density of 200×10^6 cells per 100 μl. The buffer contained 10 mM Tris–HCl (pH 7.5), 150 nM NaCl, 50 mM NaF, 1 mM ethylenediaminetetraacetic acid (EDTA), 0.5 mM Na_3VO_4, 10% glycerol, 0.5% NP-40 and 0.1 mM phenylmethylsulfonyl fluoride (PMSF). After 10-s homogenization, the resulting extracts were kept on ice for 30 min and then were centrifuged for 15 min at 2000 *g*. The supernatants from treated tumor cells were assayed for uric acid using Uric Acid C test (Wako, Osaka, Japan).

Preparation of DCs

Peripheral blood samples were obtained from normal HLA-A24 positive healthy volunteers and PBMC were isolated by sedimentation over Ficoll-Hypaque. They were subsequently allowed to adhere in culture flasks for 1 h at 37 °C at a density of 4.0×10^7 cells per plate. Non-adherent cells in the plate were removed and the remaining (adherent) cells were cultured for 7 days in AIM-V (Gibco, Rockville, MD, USA) containing 2% heated-inactivated autologous serum supplemented with GM-CSF (50 ng ml^{-1}) and IL-4 (50 ng ml^{-1}).

Cytokine production assay

DCs were co-cultured with treated tumor cells at a ratio of 3:1 (DC/tumor cell) in a culture medium containing GM-CSF (50 ng ml^{-1}) and IL-4 (50 ng ml^{-1}). After 24-h incubation, the supernatant was collected and stored at −80 °C until the assay. The concentrations of IFN-γ and IL-12 (p40 and p70) were measured with appropriate ELISA kits (BioSource, Camarillo, CA, USA).

MLTC and CTL assay

PBMCs were co-cultured with treated tumor cells at a ratio of 20:1 in the presence of IL-2 (Roche) (10 U ml^{-1}) and IL-7 (Genzyme Techne) (5 ng ml^{-1}) for 7 days. Cultured cells were then used as effector cells in a standard 4 h-^{51}Cr release assay and the percentage of lysed cells was calculated. Percent specific lysis = ((experimental cpm−spontaneous cpm)/(maximal cpm−spontaneous cpm) × 100). Supernatants from MLTC performed as above were also assayed for IFN-γ and IL-12 by ELISA assays (BioSource).

Western blot analysis

The primary antibodies against proteasome activator PA28 (ZMD353; Invitrogen, Carlsbad, CA, USA), actin (AC-40; Sigma Chemical Co., St. Louis, MO, USA) and peroxidase-linked secondary antibody (Amersham, Arlington Heights, IL, USA) were used. Cells were washed twice in cold PBS and collected, then lysed in lysis buffer (10 mM Tris (pH 7.5), 150 mM NaCl, 50 mM NaF, 1 mM EDTA, 10% glycerol and 0.5% NP40) containing proteinase inhibitors (0.1 mM PMSF and 0.5 mM Na_3VO_4). After 20 min on ice, the lysates were spun at 14 000 rpm in a microcentrifuge at 4 °C for 10 min. The supernatants were used as whole cell extracts. Protein concentration was determined using the Bio-Rad protein determination method (Bio-Rad, Richmond, CA, USA). Equal amounts (50 μg) of proteins were boiled for 5 min and electrophoresed under reducing conditions on 6–12.5% (w/v) polyacrylamide gels. Proteins were electrophoretically transferred to a Hybond-polyvinylidene difluoride transfer membranes (Amersham Life Science, Buckinghamshire, UK), and incubated with the primary antibody, followed by peroxidase-linked secondary antibody. An Amersham ECL chemiluminescent western system (Amersham) was used to detect secondary probes.

Statistical analysis
Data are expressed as mean ± s.d. The Student's *t*-test was used to compare differences. Statistical significance was defined when P was <0.05.

Acknowledgements

We thank Drs Tamotsu Yoshimori and Frank McCormick for providing pLC3-GFP plasmid and Onyx-015, respectively.
The study was supported by Grants-in-Aid from the Ministry of Education, Science and Culture, Japan; and Grants from the Ministry of Health and Welfare, Japan.

References

Aliberti J, Viola JP, Vieira-de-Abreu A, Bozza PT, Sher A, Scharfstein J. (2003). Bradykinin induces IL-12 production by dendritic cells: a danger signal that drives Th1 polarization. *J Immunol* **170**: 5349–5353.
Bartholomae WC, Rininsland FH, Eisenberg JC, Boehm BO, Lehmann PV, Tary-Lehmann M. (2004). T cell immunity induced by live, necrotic, and apoptotic tumor cells. *J Immunol* **173**: 1012–1022.
Glantzounis GK, Tsimoyiannis EC, Kappas AM, Galaris DA. (2005). Uric acid and oxidative stress. *Curr Pharm Des* **11**: 4145–4151.
Ho LJ, Wang JJ, Shaio MF, Kao CL, Chang DM, Han SW *et al*. (2001). Infection of human dendritic cells by dengue virus causes cell maturation and cytokine production. *J Immunol* **166**: 1499–1506.
Hu DE, Moore AM, Thomsen LL, Brindle KM. (2004). Uric acid promotes tumor immune rejection. *Cancer Res* **64**: 5059–5062.
Kawashima T, Kagawa S, Kobayashi N, Shirakiya Y, Umeoka T, Teraishi F *et al*. (2004). Telomerase-specific replication-selective virotherapy for human cancer. *Clin Cancer Res* **10**: 285–292.
Lenaerts L, Naesens L. (2006). Antiviral therapy for adenovirus infections. *Antiviral Res* **71**: 172–180.
Lindenmann J, Klein PA. (1967). Viral oncolysis: increased immunogenicity of host cell antigen associated with influenza virus. *J Exp Med* **126**: 93–108.
Manjili MH, Park J, Facciponte JG, Subjeck JR. (2005). HSP110 induces 'danger signals' upon interaction with antigen presenting cells and mouse mammary carcinoma. *Immunobiology* **210**: 295–303.
Shi Y, Evans JE, Rock KL. (2003). Molecular identification of a danger signal that alerts the immune system to dying cells. *Nature* **425**: 516–521.
Sijts A, Sun Y, Janek K, Kral S, Paschen A, Schadendorf D *et al*. (2002). The role of the proteasome activator PA28 in MHC class I antigen processing. *Mol Immunol* **39**: 165–169.
Steinman RM, Turley S, Mellman I, Inaba K. (2000). The induction of tolerance by dendritic cells that have captured apoptotic cells. *J Exp Med* **191**: 411–416.
Sun Y, Sijts AJ, Song M, Janek K, Nussbaum AK, Kral S *et al*. (2002). Expression of the proteasome activator PA28 rescues the presentation of a cytotoxic T lymphocyte epitope on melanoma cells. *Cancer Res* **62**: 2875–2882.
Taki M, Kagawa S, Nishizaki M, Mizuguchi H, Hayakawa T, Kyo S *et al*. (2005). Enhanced oncolysis by a tropism-modified telomerase-specific replication-selective adenoviral agent OBP-405 ('Telomelysin-RGD'). *Oncogene* **24**: 3130–3140.
Umeoka T, Kawashima T, Kagawa S, Teraishi F, Taki M, Nishizaki M *et al*. (2004). Visualization of intrathoracically disseminated solid tumors in mice with optical imaging by telomerase-specific amplification of a transferred green fluorescent protein gene. *Cancer Res* **64**: 6259–6265.
Watanabe T, Hioki M, Fujiwara T, Nishizaki M, Kagawa S, Taki M *et al*. (2006). Histone deacetylase inhibitor FR901228 enhances the antitumor effect of telomerase-specific replication-selective adenoviral agent OBP-301 in human lung cancer cells. *Exp Cell Res* **312**: 256–265.

Supplementary Information accompanies the paper on the Oncogene website (http://www.nature.com/onc).

Establishment of biological and pharmacokinetic assays of telomerase-specific replication-selective adenovirus

Yuuri Hashimoto,[1] Yuichi Watanabe,[1] Yoshiko Shirakiya,[1] Futoshi Uno,[2] Shunsuke Kagawa,[2] Hitoshi Kawamura,[1] Katsuyuki Nagai,[1] Noriaki Tanaka,[3] Horomi Kumon,[2] Yasuo Urata[1] and Toshiyoshi Fujiwara[2,4]

[1]Oncolys BioPharma, 3-16-33 Roppongi, Minato-ku, Tokyo 106-0031; [2]Center for Gene and Cell Therapy, Okayama University Hospital, 2-5-1 Shikata-cho, Okayama 700-8558; [3]Division of Surgical Oncology, Department of Surgery, Okayama University Graduate School of Medicine and Dentistry, 2-5-1 Shikata-cho, Okayama 700-8558, Japan

(Received June 25, 2007/Revised September 11, 2007/Accepted October 4, 2007/Online publication January 14, 2008)

The use of replication-selective tumor-specific viruses represents a novel approach for the treatment of neoplastic disease. We constructed an attenuated adenovirus, telomerase-specific replication-selective adenovirus (TRAD), in which the human telomerase reverse transcriptase promoter element drives the expression of the *E1A* and *E1B* genes linked with an internal ribosome entry site (IRES). Forty-eight hours after TRAD infection at a multiplicity of infection of 1.0, the cell viability of H1299 human lung cancer cells was consistently less than 50% and therefore this procedure could be used as a potency assay to assess the biological activity of TRAD. We also established a quantitative real-time polymerase chain reaction (PCR) analysis with consensus primers for either the adenovirus E1A or IRES sequence. The linear ranges of quantitation with E1A and IRES primers were 10^3–10^8 and 10^2–10^8 plaque-forming units/mL in the plasma, respectively. The PCR analysis demonstrated that the levels of *E1A* in normal tissues were more than 10^3 lower than in the tumors of A549 human lung tumor xenografts in *nu/nu* mice at 28 days after intratumoral injection. Our results suggest that the cell-killing assay against H1299 cells and real-time PCR can be used to assess the biological activity and biodistribution of TRAD in clinical trials. (*Cancer Sci* 2008; 99: 385–390)

The emerging fields of functional genomics and functional proteomics provide an expanding repertoire of clinically applicable targeted therapeutics.[(1)] Replication-selective oncolytic viruses provide a new platform for treatment of a variety of human cancers.[(2,3)] Promising clinical trials have shown the antitumor potency and safety of mutant or genetically modified adenoviruses.[(4,5)] We constructed previously an adenovirus vector, TRAD, in which the hTERT promoter element drives the expression of the *E1A* and *E1B* genes linked with an IRES. We showed that TRAD caused efficient selective killing of human cancer cells, but not normal cells.[(6)] Many studies have demonstrated that the majority of malignant tumors express telomerase activity,[(7)] suggesting that TRAD can potentially kill most human cancer cells.

TRAD can replicate and then lyse cancer cells, infect neighboring cancer cells, and subsequently induce oncolysis throughout the whole tumor mass *in vivo*. As preclinical models showed that TRAD could spread into the bloodstream, it is important to monitor carefully the amount of TRAD in the circulation after intratumoral injection of TRAD to avoid serious adverse events due to viremia. Although we used vector-specific primers that detected the p53 open reading frame–adenoviral DNA junction in a phase I clinical trial of a replication-deficient adenoviral vector expressing the wild-type *p53* gene (Advexin),[(8)] no appropriate method has been established to detect TRAD quantitatively. In addition, there is also a need for a procedure that can evaluate the biological activity of TRAD for clinical application.

In the present study, we characterized a potent antitumor viral agent, TRAD, to establish a biological assay and developed a single quantitative PCR method that can be used to assess the number of viral genomes present in the plasma as well as tissues.

Materials and Methods

Cells and culture conditions. H1299 (a human non-small-cell lung cancer cell line), H460 (a human large-cell lung cancer cell line), A549 (a human lung adenocarcinoma cell line), LNCap (a human metastatic prostate carcinoma cell line), MKN28 and MKN45 (human gastric adenocarcinoma cell lines), PC-3 (a human prostate adenocarcinoma cell line), SW620 (a human colorectal carcinoma cell line), and TE8 and T.Tn (human esophagus squamous carcinoma cell lines) were propagated to monolayer cultures in RPMI-1640 supplemented with 10% FBS, and 100 units/mL PG and 100 µg/mL SM. HeLa (a human cervical adenocarcinoma cell line), HepG2 (a human hepatocellular carcinoma cell line), Panc-1 (a human pancreatic epithelioid carcinoma cell line), and 293 (a transformed embryonic kidney cell line) were grown in DMEM containing high glucose (4.5 g/L) (high) with 10% FBS and PG/SM. HT-29 (a human colorectal adenocarcinoma cell line) was grown in McCoy's 5a with 10% FBS and PG/SM. MCF-7 (a human mammary gland adenocarcinoma cell line) was grown in Earle's Minimum Essential Medium with 10% FBS, PG/SM, and 2 mM L-glutamine. OST, SaOS2, and HOS (human osteosarcoma cell lines) were grown in DMEM (high) with 10% FBS and PG/SM. HSC-3 and HSC-4 (human tongue squamous carcinoma cell lines) were obtained from the Health Science Resources Bank (Osaka, Japan) and grown in DMEM (high) with 10% FBS and PG/SM. SCC-4 and SCC-9 (human tongue squamous carcinoma cell lines) were obtained from American Type Culture Collection (ATCC, Rockville, MD, USA) and grown in DMEM containing Nutrient Mixture (Ham's F-12) with 10% FBS, PG/SM, and 400 ng/mL hydrocortisone. U-2OS (a human osteosarcoma cell line) was obtained from ATCC and grown in McCoy's 5a with 10% FBS and PG/SM. NHLF was purchased from Takara Biomedicals (Kyoto, Japan) and cultured in the medium recommended by the manufacturer.

Recombinant adenoviruses. The recombinant replication-selective tumor-specific adenovirus vector TRAD was constructed and

[4]To whom correspondence should be addressed. E-mail: toshi_f@md.okayama-u.ac.jp
Abbreviations: ATCC, American Type Culture Collection; DMEM, Dulbecco's modified Eagle's medium; FBS, fetal bovine serum; hTERT, human telomerase reverse transcriptase; ID_{50}, the multiplicity of infection that causes 50% growth inhibition; IRES, internal ribosome entry site; NHLF, normal human lung fibroblasts; MOI, multiplicity of infection; PCR, polymerase chain reaction; PFU, plaque-forming units; PG, penicillin; SM, streptomycin; TRAD, telomerase-specific replication-selective adenovirus; XTT, sodium 3'-[1-(phenylaminocarbonyl)-3,4-tetrazolium]-bis(4-methoxy-6-nitro)benzene sulfonic acid hydrate.

doi: 10.1111/j.1349-7006.2007.00665.x

characterized as described previously.[6,9–11] The virus was purified by $CsCl_2$ step-gradient ultracentrifugation followed by $CsCl_2$ linear-gradient ultracentrifugation. The virus particle titer and infectious titer were determined spectrophotometrically and by plaque assay, respectively, in 293 cells.

Cell-viability assay. The XTT assay was carried out to measure cell viability. Cells were plated on 96-well plates at 1×10^3 cells/well 20 h before viral infection. HSC-4, SCC-4, and SCC-9 cells were then infected with TRAD at MOI of 0, 1, 10, and 50 PFU/cell. Other cell lines were infected with TRAD at MOI of 0, 0.1, 1, and 10 PFU/cell. Cell viability was determined at 1, 2, 3, and 5 days after virus infection using Cell Proliferation Kit II (Roche Molecular Biochemicals, Indianapolis, IN, USA) according to the protocol provided by the manufacturer. Using the cell viability data at 3 days after virus infection, we determined the TRAD ID_{50} of each cell line.

Cell-killing assay. H1299 cells were plated at 5×10^4 cells/well on 24-well plates and infected with TRAD at MOI of 0, 0.01, 0.1, 1, and 10 PFU/cell. Forty-eight hours later, the number of cells in each well was counted. Experiments were carried out in triplicate for each MOI, and cell viability was assessed by the trypan blue dye exclusion assay.

Quantitative real-time PCR assay. Viral DNA from serially diluted viral stocks and tumor cells infected with TRAD were extracted using QIAamp DNA Mini Kit (Qiagen, Valencia, CA, USA), and quantitative real-time PCR assay for either the *E1A* gene or the IRES sequence was carried out using a LightCycler instrument and a LightCycler DNA Master SYBR Green I kit (Roche Molecular Biochemicals). Typical amplification mixes (20 µL) contained 3 mM $MgCl_2$, 0.3 µM of each primer for IRES or 0.5 µM for *E1A*, and 2 µL of 10 × LightCycler FastStart DNA Master SYBR Green I. The sequences of the specific primers used in this experiment were: IRES, 5′-GAT TTT CCA CCA TAT TGC CG-3′ and 5′-TTC ACG ACA TTC AAC AGA CC-3′; E1A, 5′-CCT GTG TCT AGA GAA TGC AA-3′ and 5′-ACA GCT CAA GTC CAA AGG TT-3′. PCR amplifications were carried out in glass capillary tubes. PCR amplification for IRES began with a 10-min denaturation step at 95°C and then 40 cycles of denaturation at 95°C for 10 s, annealing at 60°C for 10 s, and extension at 72°C for 6 s. PCR amplification for *E1A* began with a 10-min denaturation step at 95°C and then 40 cycles of denaturation at 95°C for 10 s, annealing at 58°C for 15 s, and extension at 72°C for 8 s. Data analysis was carried out using LightCycler Software (Roche Molecular Biochemicals).

***In vivo* human tumor model.** A549 human lung cancer cells (5×10^6 cells/mouse) were injected subcutaneously into the flank of 7- to 9-week-old female BALB/c *nu/nu* mice and permitted to grow to approximately 5–6 mm in diameter. At that stage, a 100-µL solution containing 1×10^8 PFU of TRAD was injected into the tumor. The tumors and organs were harvested 28 and 70 days later and DNA was extracted from each tissue. To compare viral replication in the tumor and other normal organs, quantitative real-time PCR for the *E1A* gene was carried out using a LightCycler instrument. The experimental protocol was approved by the Ethics Review Committee for Animal Experimentation of Okayama University School of Medicine.

Statistical analysis. All data were expressed as mean ± SD. Differences between groups were examined for statistical significance using Student's *t*-test. A *P*-value less than 0.05 denoted the presence of a statistically significant difference.

Results

***In vitro* cytopathic efficacy of TRAD in human cancer cell lines derived from different organs.** To determine whether TRAD infection induces broad-spectrum selective cell lysis, 23 tumor cell lines derived from 11 different organs (head and neck, lung, esophagus, stomach, colon, liver, pancreas, breast, prostate, uterus, and bone) were infected with TRAD at various MOI. Previous studies using a real-time reverse transcription-PCR method have demonstrated that these cell lines express detectable levels of hTERT mRNA.[6,9] Cytotoxicity was then assessed using the XTT cell-viability assay over 5 days after infection. As shown in Figure 1a, TRAD infection induced cell death in all cell lines except T.Tn esophageal cancer cells in a dose-dependent manner. Calculated ID_{50} values confirmed that all cell lines except T.Tn could be killed efficiently by TRAD at an MOI of less than 25 (Fig. 1b). These results suggest the broad-spectrum antitumor potency of TRAD.

Establishment of a standard assay to assess the biological activity of TRAD. H1299 human lung cancer cells and LNCap human prostate cancer cells were the most sensitive cell lines to TRAD-induced cell death (Fig. 1b). Accordingly, we used H1299 cells to evaluate the biological activity of TRAD. To test whether the selective replication of TRAD translates into selective oncolysis, we compared the cytopathic effects of TRAD in H1299 cells and NHLF at 5 days after infection. The dose–response curve of the relative cell viability in H1299 cells was shifted to the left compared to that in NHLF, suggesting that TRAD killed H1299 cells 10^2–10^3 more efficiently than NHLF (Fig. 2a).

We next determined the minimal dose of TRAD that could induce more than 50% of cell death in H1299 cells. As shown in Figure 2b, the cell viability of H1299 cells was less than 40% at 48 h after their infection with TRAD at a MOI of 1.0, but was 60% after infection with a MOI of 0.1. We also confirmed that H1299 cells at various passages (5th to 20th after purchase from ATCC) could be killed by TRAD in a similar fashion (data not shown). Therefore, TRAD could be considered biologically active, if TRAD at a MOI of 1 reduces the cell viability of H1299 cells by more than 50% at 48 h after infection. To estimate the utility of this assay, we examined the biological activity of heat-inactivated TRAD. Infection with intact TRAD at a MOI of 10 induced approximately 90% reduction in H1299 cell viability at 48 h after infection, whereas the antitumor activity was completely inhibited when it was preheated at 56°C for 5 or 10 min (Fig. 2c).

Development of quantitative PCR assay to detect copy numbers of TRAD. We used real-time PCR for quantitative detection of TRAD. Oligonucleotide primers were designed to achieve DNA amplification of the adenoviral E1A or IRES sequences in the TRAD genome (Fig. 3a). To generate accurate standard curves, TRAD at a known concentration was serially diluted and used as a template for real-time PCR analysis. Detection of IRES and E1A genome copies was achieved consistently and reproducibly by the PCR cycle values used. A linear relationship could be obtained between the number of cycles and the $\log_{10}$ dilution when 10^2–10^8 IRES copies and 10^3–10^8 E1A copies were assayed. Regression analysis of IRES and E1A curves resulted in very high correlation coefficients (0.99 and 1.00, respectively) for these concentration ranges (Fig. 3b). In addition, the dilution of TRAD virus in the plasma did not affect the sensitivity and dynamic ranges of quantification (Fig. 3b), suggesting that this method can be used to detect TRAD in the blood circulation.

***In vitro* quantification and replication monitoring of TRAD in infected human tumor and normal cells.** We next examined the replication ability of TRAD in different cell lines by measuring the relative amounts of IRES and E1A copy numbers. LNCap and NHLF cells were harvested at the indicated time points over 5 and 7 days, respectively, after infection with TRAD, and subjected to quantitative real-time PCR analysis using IRES and E1A primers. The ratios were normalized by dividing the value of cells obtained at 2 h after viral infection. As shown in Figure 4a, TRAD replicated 10^3–10^4 by 5 days after infection; its replication, however, was attenuated to less than 10^3 in normal NHLF cells. We previously reported that TRAD could replicate 10^5–10^6 by 3 days after infection in H1299 cells;[6,10] however, as

doi: 10.1111/j.1349-7006.2007.00665.x

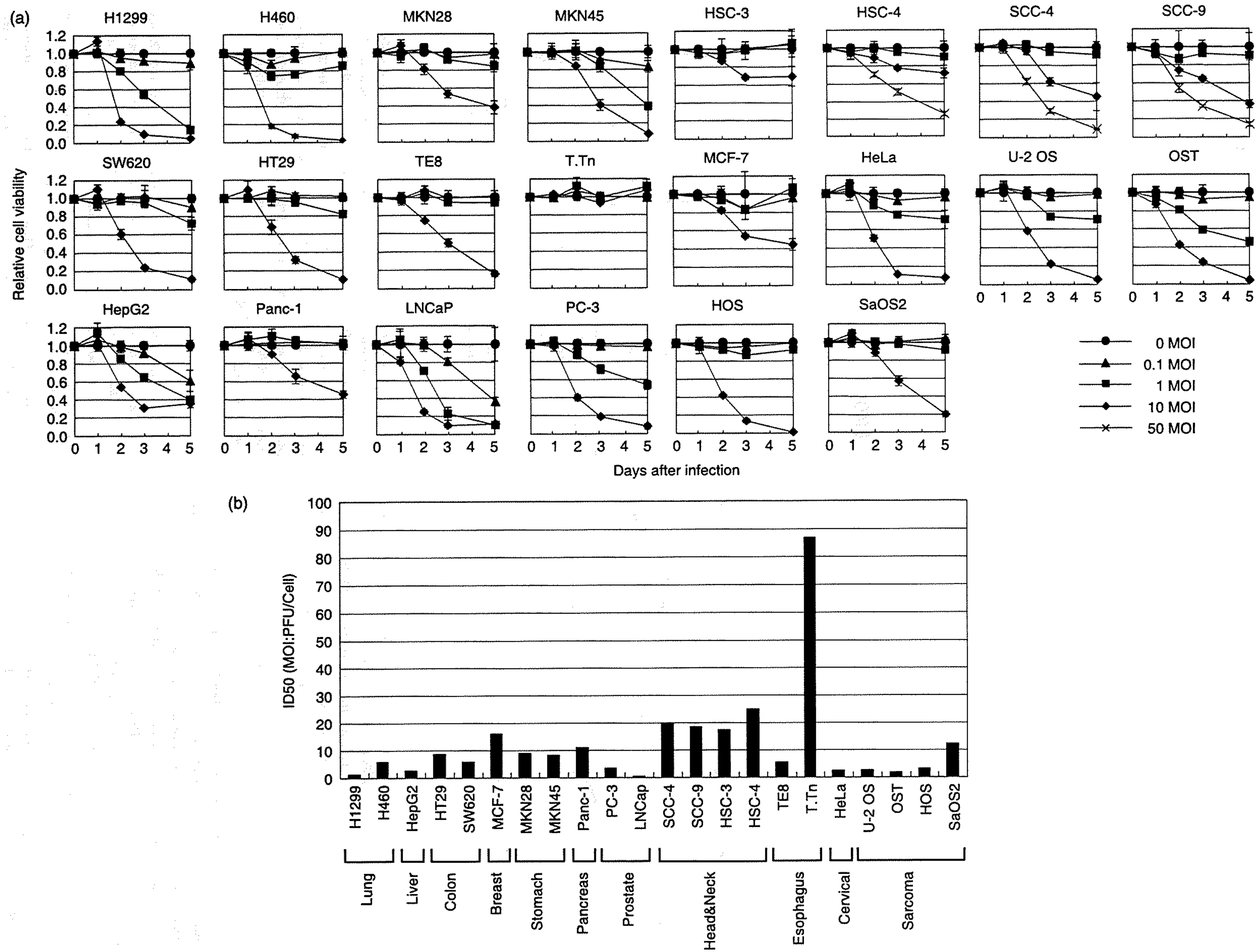

Fig. 1. Oncolytic effects of telomerase-specific replication-selective adenovirus (TRAD) *in vitro* on a variety of human cancer cell lines. (a) Cells were infected with TRAD at indicated multiplicity of infection (MOI) values, and surviving cells were quantitated over 5 days by XTT assay. Data are mean ± SD. (b) The 50% inhibiting doses of TRAD on cell viability at 3 days after infection were calculated and expressed as ID_{50} values. PFU, plaque-forming units; XXT, sodium 3′-[1-(phenylaminocarbonyl)-3,4-tetrazolium]-bis(4-methoxy-6-nitro)benzene sulfonic acid hydrate.

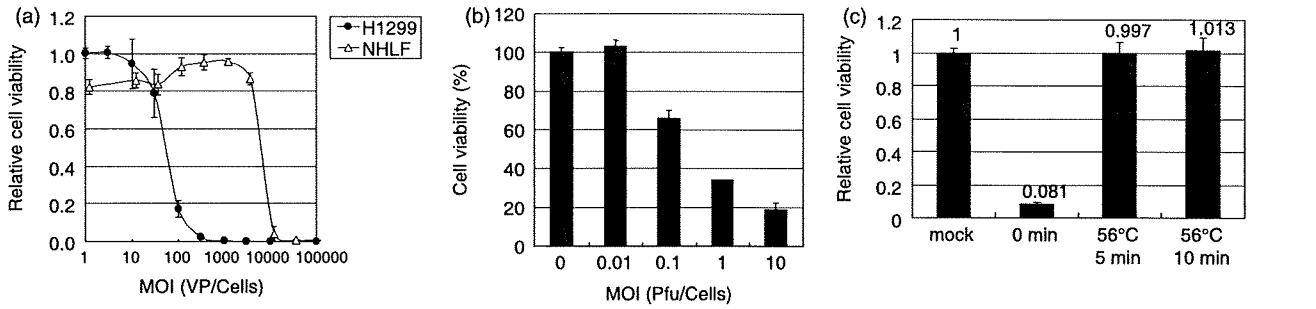

Fig. 2. Antitumor effects of telomerase-specific replication-selective adenovirus (TRAD) on H1299 non-small-cell lung cancer cells *in vitro*. (a) Effects of various concentrations of TRAD on H1299 cancer cells and normal human lung fibroblasts (NHLF) assessed at 5 days after treatment with XTT assay. Results are expressed as the percentage of untreated control. (b) H1299 cells were cultured as monolayers in triplicate in 24-well culture plates, infected with TRAD at the indicated multiplicities of infection (MOI), and assessed for cell viability 48 h after infection. Mock-infected cells were used as a control. (c) H1299 cells were plated on 96-well plates and infected with 10 MOI of TRAD heated at 56°C for 5 or 10 min, or non-treated TRAD. An XTT assay was carried out at 3 days after virus infection. Mock-infected cells were used as a control. Data represent the mean ± SD of triplicate experiments. PFU, plaque-forming units; XXT, sodium 3′-[1-(phenylaminocarbonyl)-3,4-tetrazolium]-bis(4-methoxy-6-nitro) benzene sulfonic acid hydrate; VP, virus particles.

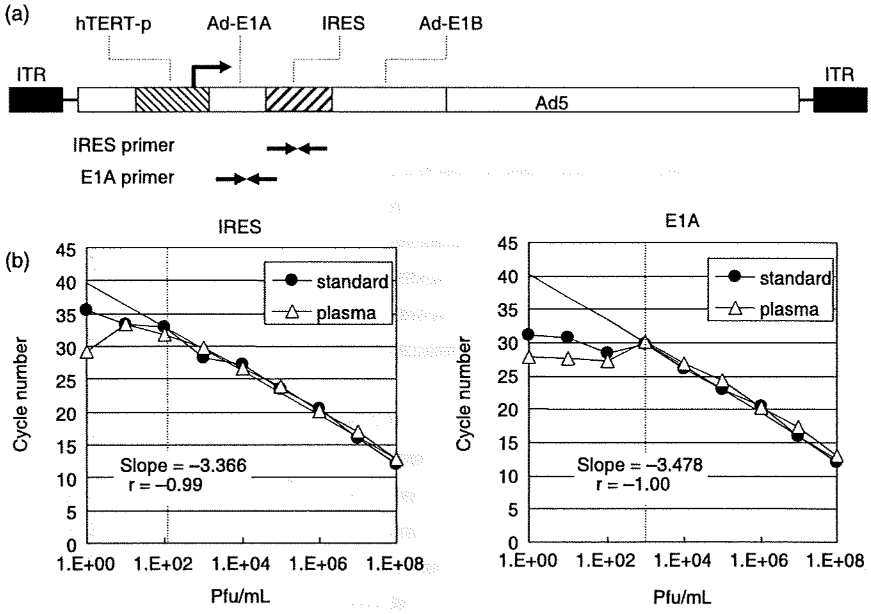

Fig. 3. Detection of normal human lung fibroblasts (TRAD) using quantitative polymerase chain reaction (PCR) assay. (a) Schematic diagram of the DNA structure of TRAD. TRAD contains the human telomerase reverse transcriptase (hTERT) promoter sequence inserted into the adenovirus genome to drive transcription of the *E1A* and *E1B* bicistronic cassette linked by the internal ribosome entry site (IRES) structure. Sites to which PCR primers (IRES and E1A) were targeted are indicated. Two primer pairs of IRES and E1A were designed to detect the TRAD genome. (b) Standard calibration curves of threshold cycle values and copy numbers are shown using serial dilution of TRAD virus stock. The coefficient of correlation (r^2) and slope are indicated for assays with IRES and E1A primers. ITR, inverted terminal repeats; PFU, plaque-forming units.

LNCap cells were more sensitive to TRAD-mediated cytotoxicity than H1299 cells (Fig. 1a), viral replication reached a plateau phase around 10^4 when LNCap cells started to die. Moreover, PCR targeting IRES and E1A showed similar replication profiles for TRAD in MCF-7 human breast cancer cells (Fig. 4b). To monitor the long-term viral replication, MCF-7 cells that were less sensitive to the cytopathic effect of the virus were used.

***In vivo* determination of TRAD genomes in tissue samples after intratumoral injection.** To evaluate selective replication of TRAD *in vivo*, we examined mouse tissues, including implanted tumors, for the presence of viral DNA by quantitative real-time PCR, following intratumoral viral injection. Mice with established subcutaneous A549 human lung tumor xenografts received a single intratumoral injection of 1×10^8 PFU of TRAD, and were killed 28 or 70 days after injection. To obtain the sufficient amounts of tumor tissues for analysis, we chose to use A549 cells. Our preliminary experiments demonstrated that intratumoral administration of TRAD suppressed tumor growth significantly compared with mock-treated tumors at 42 days after initiation of treatment ($P < 0.05$); however, the *in vivo* antitumor effect against A549 tumors was less than that against H1299 or LNCap tumors (data not shown). Although E1A DNA was detected in serum and some normal tissues examined (brain, heart, lung, ovary, liver, uterus, kidneys, bladder, colon, and axillary and mesenteric lymph nodes), tumors injected with TRAD contained at least 1000-fold more *E1A* copies (Fig. 5). These results suggest that quantitative real-time PCR allows detection and quantification of the number of TRAD genomes present in tissue samples after intratumoral injection of TRAD *in vivo*.

Discussion

Oncolytic viruses have been developed as anticancer agents based on the advantage of selective killing of tumor cells by controlled replication of the virus in the tumors, resulting in minimal undesired effects on normal cells.[2] Furthermore, amplified viruses can infect adjacent tumor cells as well as reach distant metastatic tumors through the blood circulation. Alhtough this might be a potential advantage of oncolytic viruses, systemic dissemination of large amounts of virus may induce virus-related symptoms including fever, diarrhea, pneumonia, and hepatitis, eventually leading to death. Therefore, virus shedding and distribution have to be evaluated by appropriate and suitable methods. In addition,

doi: 10.1111/j.1349-7006.2007.00665.x

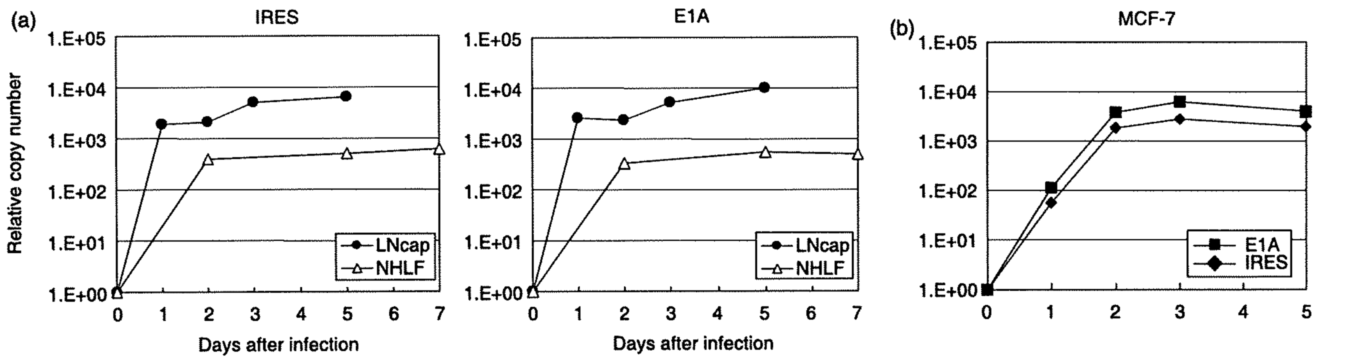

Fig. 4. Quantitative measurement of viral DNA replication in human cancer and normal cells *in vitro* by quantitative polymerase chain reaction (PCR) assay. (a) LNCap human prostate cancer cells and normal human lung fibroblast (NHLF) cells were infected with telomerase-specific replication-selective adenovirus (TRAD) at a multiplicity of infection (MOI) of 1 for 2 h. Following the removal of virus inoculum, cells were further incubated for the indicated periods of time, and then subjected to the real-time quantitative PCR assay. The amounts of viral internal ribosome entry site (IRES) and E1A copy number was defined as the fold increase for each sample relative to that at 2 h (2 h equals 1). (b) MCF-7 human breast cancer cells were infected with TRAD at a MOI of 1 and subjected to the PCR assay at the indicated time points. The relative TRAD DNA levels detected by IRES and E1A primers were plotted.

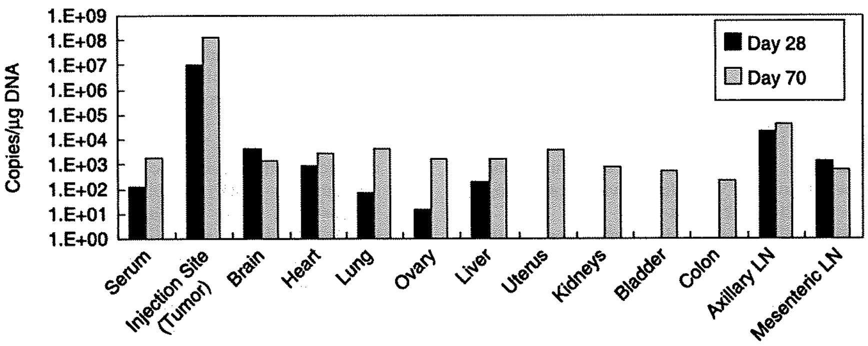

Fig. 5. Spread and replication of telomerase-specific replication-selective adenovirus (TRAD) following intratumoral administration in *nu/nμ* mice transplanted with A549 tumor cells. A549 tumor cells were injected subcutaneously into the right flank of mice at 5×10^6 cells/mouse. Mice received intratumoral injection of 1×10^8 plaque-forming units of TRAD when the tumor reached a size of approximately 5–6 mm in diameter. DNA was extracted from the subcutaneous tumor and various tissues of *nu/nμ* mice at 28 or 70 days after infection. Viral DNA was detected by quantitative polymerase chain reaction amplification of the adenoviral E1A sequence. The amounts of TRAD genome were defined as viral E1A copy number per μg DNA. LN, lymph nodes.

to avoid unexpected infectious disease due to viral overdose, we need assays that accurately detect the biological activity of viruses. In the present study, for clinical trials of TRAD, we developed an assay designed to estimate the biological activity of TRAD and to detect the copy number of TRAD in the plasma as well as tissues.

Although telomerase-specific TRAD exhibited a broad cytopathic effect against human cancer cell lines of different tissue origins, a human non-small-cell lung cancer cell line, H1299, was chosen for the biological assay of TRAD. H1299 was one of the most sensitive cell lines to TRAD-mediated cell death ($ID_{50} = 0.94$ MOI) and could be killed efficiently by TRAD infection in a dose-dependent fashion (Fig. 1). Because H1299 cells can be obtained from ATCC, they can be used in clinical laboratories to assess the biological activity of TRAD with a qualified standard protocol. In addition, although adenoviral E1B-55 kDa protein is known to bind to the tumor suppressor p53 protein,[12] H1299 cells are p53-null and therefore the interaction of E1B-55 kDa with p53, which in turn results in transcriptional modulation, can be ignored in this cell line. Thus, H1299 is considered an appropriate cell line for assessment of TRAD activity in certain preparations. In the present study, we considered TRAD to be active when the viability of H1299 cells was reduced by more than 50% at 48 h after TRAD infection at an MOI of 1. Using this biological assay, we confirmed that heat treatment of aliquots of TRAD at 56°C for 5 min is sufficient to inactivate its antitumor potential (Fig. 2c). These results advocate the use of the H1299 cell-based cytotoxicity assay as a standard method for quantitative assessment of the biological activity of TRAD in virus stocks for clinical trials.

Various biological methods, such as determination of infectious units in plaque assays, have been used routinely in clinical trials to monitor viral loads in the peripheral circulation.[8] These methods are useful for evaluating safety because the viral titers directly reflect the infectivity of viruses. However, because the plaque assay consists of labor-intensive and time-consuming steps, real-time monitoring of the biodistribution of the virus might be difficult. Here we described the development of a quantitative real-time PCR assay that can accurately quantify genome copy numbers of TRAD over a large linear range. Using primers targeting TRAD-specific sequences, such as adenoviral E1A and IRES, real-time PCR could accurately detect the number of TRAD genomes in the plasma as well as in the cells (Figs 3,4). The assay showed that TRAD replicated even in NHLF, although the level was much lower than that in tumor cells. It is usually difficult to maintain the normal cells primarily isolated from human tissues such as human hepatocytes in the culture; however, commercially available NHLF could be cultured for several passages, suggesting that NHLF may have some characteristics different from primary isolated normal cells, including telomerase activity. We also found that the number of viral genomes could be measured in genomic DNA purified from tissues of mice *in vivo* after injection of TRAD into the xenografts (Fig. 5). Although viral DNA could be detected even in normal tissues 70 days after intratumoral injection of TRAD, the absence of infectious virus as assessed by the plaque assay suggests that there are only DNA fragments in tissues. Our preliminary experiments have demonstrated that DNA could be isolated from tumors as small as 5 mm in diameter (data not shown). Therefore, the real-time PCR method with E1A and IRES primers permits rapid and quantitative detection of TRAD DNA in clinical samples.

We have shown recently the antiviral activity of cidofovir against TRAD *in vitro*. Cidofovir is an acyclic nucleoside phosphonate with potent broad-spectrum anti-DNA viral activity and has been approved for the treatment of many types of viruses, including cytomegalovirus and adenovirus.[13] Although viremia after TRAD administration is extremely rare because of the anti-adenovirus antibodies expected to be present in most patients, a real-time PCR-based pharmacokinetic assay can allow the early detection of disseminated virus, and thus its use could provide an indication for commencement of cidofovir treatment in clinical trials.

In summary, we have established a fast, reliable, and sensitive assay to assess the biological activity of TRAD *in vitro* and to detect the viral genome in the plasma as well as tissues *in vivo*. A phase I clinical trial of TRAD targeting advanced solid tumors is currently underway in the USA following the approval of the Food and Drug Administration. Such an assay has been used in this ongoing trial and the data will be analyzed in the near future for the assessment of the safety, efficacy, and biodistribution of TRAD.

Acknowledgments

This work was supported in part by grants from the Ministry of Education, Science, and Culture, Japan, and by grants from the Ministry of Health and Welfare, Japan.

References

1 Kohn EC, Lu Y, Wang H *et al.* Molecular therapeutics: promise and challenges. *Semin Oncol* 2004; **31**: 39–53.
2 Hawkins LK, Lemoine NR, Kirn D. Oncolytic biotherapy: a novel therapeutic platform. *Lancet Oncol* 2002; **3**: 17–26.
3 Chiocca EA. Oncolytic viruses. *Nat Rev Cancer* 2002; **2**: 938–50.
4 Reid T, Galanis E, Abbruzzese J *et al.* Hepatic arterial infusion of a replication-selective oncolytic adenovirus (dl1520): phase II viral, immunologic, and clinical endpoints. *Cancer Res* 2002; **62**: 6070–9.
5 Hamid O, Varterasian ML, Wadler S *et al.* Phase II trial of intravenous CI-1042 in patients with metastatic colorectal cancer. *J Clin Oncol* 2003; **21**: 1498–504.
6 Kawashima T, Kagawa S, Kobayashi N *et al.* Telomerase-specific replication-selective virotherapy for human cancer. *Clin Cancer Res* 2004; **10**: 285–92.
7 Kim NW, Piatyszek MA, Prowse KR *et al.* Specific association of human telomerase activity with immortal cells and cancer. *Science* 1994; **266**: 2011–15.
8 Fujiwara T, Tanaka N, Kanazawa S *et al.* Multicenter phase I study of repeated intratumoral delivery of adenoviral p53 in patients with advanced non-small-cell lung cancer. *J Clin Oncol* 2006; **24**: 1689–99.
9 Umeoka T, Kawashima T, Kagawa S *et al.* Visualization of intrathoracically disseminated solid tumors in mice with optical imaging by telomerase-specific amplification of a transferred green fluorescent protein gene. *Cancer Res* 2004; **64**: 6259–65.
10 Taki M, Kagawa S, Nishizaki M *et al.* Enhanced oncolysis by a tropism-modified telomerase-specific replication-selective adenoviral agent OBP-405 ('Telomelysin-RGD'). *Oncogene* 2005; **24**: 3130–40.
11 Watanabe T, Hioki M, Fujiwara T *et al.* Histone deacetylase inhibitor FR901228 enhances the antitumor effect of telomerase-specific replication-selective adenoviral agent TRAD in human lung cancer cells. *Exp Cell Res* 2006; **312**: 256–65.
12 Cathomen T, Weitzman MD. A functional complex of adenovirus proteins E1B-55kDa and E4orf6 is necessary to modulate the expression level of p53 but not its transcriptional activity. *J Virol* 2000; **74**: 11 407–12.
13 Ouchi M, Kawamura H, Nagai K, Urata Y, Fujiwara T. Antiviral activity of cidofovir against telomerase-specific replication-competent adenovirus, Telomelysin (OBP-301). *Mol Ther* 2007; **15** (Suppl 1): S173.

doi: 10.1111/j.1349-7006.2007.00665.x

Int. J. Cancer: **122**, 2628–2633 (2008)

Combination of oncolytic adenovirotherapy and Bax gene therapy in human cancer xenografted models. Potential merits and hurdles for combination therapy

Masayoshi Hioki[1,2], Shunsuke Kagawa[1,2*], Toshiya Fujiwara[1,2], Ryo Sakai[1,2], Toru Kojima[1,2], Yuichi Watanabe[1,3], Yuuri Hashimoto[3], Futoshi Uno[1,2], Noriaki Tanaka[1] and Toshiyoshi Fujiwara[1,2]

[1]*Division of Surgical Oncology, Department of Surgery, Okayama University Graduate School of Medicine, Dentistry and Pharmaceutical Sciences, 2-5-1 Shikata-cho, Okayama 700-8558, Japan*
[2]*Center for Gene and Cell Therapy, Okayama University Hospital, Okayama, Japan*
[3]*Oncolys BioPharma, Inc., Tokyo, Japan*

Cancer gene therapy and oncolytic virotherapy have been studied extensively. However, their clinical application is hampered by their weak anticancer activity. We previously constructed a replicating adenovirus (OBP-301, Telomelysin), in which the human telomerase reverse transcriptase (hTERT) promoter drives expression of the adenoviral E1 genes, and causes selective lysis of human cancer cells. We hypothesized that combination adenoviral therapy containing OBP-301 and a nonreplicating adenovirus expressing the proapoptotic Bax gene could overcome the weakness and augment the anticancer efficacy of each modality. Combination treatment resulted in marked Bax protein expression and enhanced efficacy in *in vitro* cell viability assay, when compared with either single treatment. However, combination treatment was not as effective in suppressing both subcutaneous and pleural disseminated tumors compared with OBP-301 treatment alone. Further investigation revealed that combination treatment resulted in suppressed E1A protein expression associated with reduced viral replication. Our results suggest that Bax gene therapy in combination with oncolytic adenovirotherapy potentially augments their antitumor activity, but further improvements may be required to maximize the combinatorial effect *in vivo*, for the Bax gene expression to avoid interference with production of the oncolytic virus.
© 2008 Wiley-Liss, Inc.

Key words: gene therapy; oncolytic virus; bax; adenovirus

Oncolytic adenoviruses that can selectively replicate in tumor cells and cause lysis of infected cells have been extensively investigated as novel anticancer agents.[1,2] Recently, such vectors have been approved for clinical trials.[3–8] However, preclinical and clinical studies have revealed that the clinical application of these agents is hampered by their weak anticancer activity. Therefore, the development of strategies that maximize their anticancer activity is essential to the success of these agents in treating cancer.

One of the approaches to overcome this weakness is combination therapy of the oncolytic virus with a virus expressing therapeutic genes such as proapoptotic genes to augment the killing effect on cancer cells, which may lead to the future development of an arming oncolytic virus as a cancer therapeutic.

Bax is a strong proapoptotic gene that causes cytochrome C release from mitochondria, activates the caspase pathway and leads to apoptosis.[9,10] We previously constructed a binary adenoviral vector system (Ad/PGK-GV16 + Ad/GT-Bax: Ad/Bax) for Bax overexpression[11] that can transfer the Bax gene to cancer cells *in vitro* and *in vivo* and induce effective apoptosis.[12,13] However, because this system consists of E1-deleted, replication-defective adenovirus, its cell killing activity is theoretically limited to the transduced cells.

We also constructed a novel oncolytic adenovirus (OBP-301, Telomelysin), in which the human telomerase reverse transcriptase (hTERT) promoter drives expression of the adenoviral E1 genes. OBP-301 thus replicates preferentially in human cancer cells and causes their selective lysis.[14] However, as this virus also does not contain any therapeutic genes, clinical weakness is anticipated.

We hypothesize that Bax gene therapy in combination with an onlytic adenovirus could augment anticancer efficacy by overcoming the weakness of each modality. The replication-defective adenovirus with E1 deletion can become replication-competent when cotransduced with an oncolytic adenovirus supplying E1 *in trans*. Thus, the expression of the Bax gene and the viral copies would increase, which facilitates cancer cells to undergo apoptosis, release virus progenies and further spread them within the tumor.

In this study, we evaluated the transgene expression, viral replication and antitumor effect of Bax gene therapy combined with OBP-301 oncolytic adenovirotherapy in human cancer cell lines.

Material and methods

Cell lines and cell culture

Human bronchioloalveolar carcinoma A549 cells were propagated in a monolayer culture in Dulbecco's modified Eagle's medium containing Ham's F-12 nutrient mixture supplemented with 10% fetal calf serum (FCS) and antibiotics. Human gastric cancer MKN45 cells were cultured in RPMI 1640 medium containing 10% FCS and antibiotics. The cells were cultured at 37°C in a humidified incubator containing 5% CO_2.

Recombinant adenoviruses

The recombinant replication-selective, tumor-specific adenovirus vector OBP-301 (Telomelysin), and nonreplicating E1-deleted binary adenovirus vector system expressing the proapoptotic Bax gene (Ad/PGK-GV16 + Ad/GT-Bax: Ad/Bax) were previously constructed and characterized.[11,14] In a binary vector system, expression of the *Bax* gene can be induced by transferring Ad/GT-Bax into target cells along with Ad/PGK-GV16 at a ratio of 1:1. All of the viruses were propagated in a package containing 293 cells and purified by $CsCl_2$ step gradient ultracentrifugation followed by $CsCl_2$ linear gradient ultracentrifugation. Determination of virus particle titer and infectious titer (plaque-forming unit: PFU) was accomplished spectrophotometrically by the method of Maizel *et al.*[15] and by the method of Kanegae *et al.*,[16] respectively. The particles: plaque ratios were between 23:1 and 35:1.

Cell viability assay

Cells were plated in 96-well plates at a density of 1,000 cells/well and infected with OBP-301 alone, Ad/Bax alone, or their combination 15 hr later. Cell viability was assessed using a colorimetric XTT assay with the Cell Proliferation Kit II (Roche Molecular Biochemicals, Indianapolis, IN) according to the manufacturer's protocol. We determined the combination index (CI) at

This article contains supplementary material available via the Internet at http://www.interscience.wiley.com/jpages/0020-7136/suppmat.

Grant sponsors: Ministry of Education, Culture, Sports, Science and Technology of Japan, Ministry of Health, Labour and Welfare of Japan.

***Correspondence to:** Center for Gene and Cell Therapy, Okayama University Hospital, 2-5-1 Shikata-cho, Okayama 700-8558, Japan. Fax: +81-86-235-7884. E-mail: skagawa@md.okayama-u.ac.jp

Received 8 May 2007; Accepted after revision 5 December 2007
DOI 10.1002/ijc.23438
Published online 13 March 2008 in Wiley InterScience (www.interscience.wiley.com).

Publication of the International Union Against Cancer
UICC global cancer control